NASA Technical Memorandum 101631

AERODYNAMIC PARAMETERS OF AN ADVANCED
FIGHTER AIRCRAFT ESTIMATED FROM FLIGHT
DATA. PRELIMINARY RESULTS

VLADISLAV KLEIN

KEVIN P. BRENEMAN

THOMAS P. RATVASKY

JULY 1989

NASA

National Aeronautics and
Space Administration

Langley Research Center
Hampton, Virginia 23665

SUMMARY

Preliminary estimates of aerodynamic parameters of an advanced fighter aircraft were obtained from flight data of different values of the angle of attack from 8° to 54°. The data were analyzed by a stepwise regression with the ordinary least squares technique. The estimated parameters, in the form of stability and control derivatives, are plotted against the angle of attack and compared with wind tunnel measurement and previous flight results. The resulting parameters exhibit, in general, large scatter caused mainly by insufficient excitation of aircraft responses. The report also includes the data compatibility check of measured data. The effect of various input forms is demonstrated in two examples using simulated data. Based on the experience obtained, proposals are made for the future experiment for obtaining accurate parameter estimates.

SYMBOLS AND ABBREVIATIONS

a_x, a_y, a_z longitudinal, lateral, and vertical acceleration, g units

b wing span, m

b_z constant bias error in variable z

C_a general aerodynamic force and moment coefficient

C_ℓ, C_m, C_n rolling-, pitching-, and yawing-moment coefficient

C_Y, C_Z lateral- and vertical-force coefficient

$\bar{c}$ wing mean aerodynamic chord, m

g acceleration due to gravity, m/sec^2

I_X, I_Y, I_Z moments of inertia about longitudinal, lateral, and vertical body axes, $kg-m^2$

I_{XZ} product of inertia, $kg-m^2$

m mass, kg

N number of data points

n measurement-noise vector

p, q, r roll rate, pitch rate, and yaw rate, rad/sec or deg/sec

$\bar{q}$ dynamic pressure, $\rho V^2/2$, Pa

R measurement-noise covariance matrix

R^2 squared multiple correlation coefficient

S wing area, m^2

$s(\cdot)$ standard error

s^2 variance estimate

t time, sec

u, v, w longitudinal, lateral, and vertical airspeed component, m/sec

V airspeed, m/sec

X matrix of regressors

x vector of state variables or regressors

Y	vector of dependent variables
y	dependent variable
Z	vector of output variables
α	angle of attack, rad or deg
β	sideslip angle, rad or deg
δ_A	input variable expressing combined effect of aileron and differential tail and trailing edge flaps, rad or deg
δ_a, δ_r	aileron and rudder deflection, rad or deg
$\delta_{dh}, \delta_{df}, \delta_{d\ell f}$	differential tail and trailing and leading edge flap deflection, rad or deg
δ_H	input variable expressing combined effect of horizontal tail, leading and trailing edge flap deflection, rad or deg
$\delta_h, \delta_f, \delta_{\ell f}$	horizontal tail and trailing and leading edge flap deflection, rad or deg
η	vector of input variables
η_a, η_h, η_r	stick deflection in roll and pitch, and rudder pedal deflection, in
Θ	vector of unknown parameters
Θ_0, Θ_j	unknown parameters
θ, ϕ, ψ	pitch, roll, and yaw angle, rad or deg
λ_z	scale factor error of variable z
ν	vector of residuals
ρ	air density, kg/m^3

Abbreviations:

c.g.	center of gravity
m.a.c.	mean aerodynamic chord

Subscript:

    E   measured value

Superscript:

    ^   estimated value

Matrix exponent:

    T   transpose matrix

    -1   inverse matrix

Derivatives of aerodynamic coefficients $C_a (a = Y, Z, \ell, m, n)$ referenced to a system of body axes with the origin at the airplane center of gravity:

$$C_{a_p} = \frac{\partial C_a}{\partial \frac{pb}{2V}} \qquad\qquad C_{a_q} = \frac{\partial C_a}{\partial \frac{q\bar{c}}{2V}} \qquad\qquad C_{a_r} = \frac{\partial C_a}{\partial \frac{rb}{2V}}$$

$$C_{a_\alpha} = \frac{\partial C_a}{\partial \alpha} \qquad\qquad C_{a_\beta} = \frac{\partial C_a}{\partial \beta}$$

$$C_{a_{\delta j}} = \frac{\partial C_a}{\partial \delta_j} \quad , \quad j = A, a, df, dh, d\ell f, f, H, h, \ell f, r$$

INTRODUCTION

In 1988, NASA initiated the High-Alpha Technology Program in order to accelerate the development of technologies which would expand high angle-of-attack capabilities of future fighter aircraft. The flight research portion of the program has been using the F-18A High Angle-of-Attack Research Vehicle (HARV) as a flight research testbed. One of the objectives of the flight program is to obtain the high-alpha database for validation of wind tunnel and theoretical predictions and for postulating a mathematical model of the aircraft. For that reason the first set of flights included several longitudinal and lateral transient maneuvers intended for estimation of aircraft aerodynamic parameters using system identification methodology.

The purpose of this report is to summarize the preliminary results from the analysis, assess the accuracy of the instrumentation system and parameter estimates, and consider possible changes in the design of future experiments. The report starts with the description of the aircraft and flight and wind tunnel data available. Then, procedures for data analysis are briefly outlined. The results presented include checks on compatibility of measured responses, variation of estimated aerodynamic parameters with the angle of attack, and the comparison of these estimates with wind tunnel measurements and a limited number of previous flight results. Finally, a possible selection of different input forms and their effect on parameter accuracy is discussed.

AIRCRAFT

The test vehicle is a twin engine, single seat fighter aircraft. It has a moderately swept wing with highly swept leading-edge extension (LEX). The all-moving horizontal tail surfaces are mounted behind and below the wing, twin vertical tails are canted and toed out. The aircraft is controlled by four digital computers working in parallel. The computers are used in conjunction with redundant electrohydraulic servoactuators and analog sensors to provide two fail operate primary control capabilities. There is also a backup mechanical control of the stabilator surfaces and open-loop analog control of the aileron and rudder. Longitudinal control uses symmetric deflections of the stabilator, leading and trailing edge flaps. Lateral control is provided by the ailerons, differential deflections of the stabilator, leading and trailing edge flaps, and synchronous rudder deflection. A drawing of the aircraft is presented in figure 1. The basic geometric, mass, and inertia characteristics are summarized in table I. A more detailed description of the aircraft and its control system is contained in references 1 and 2.

The tested aircraft was modified by adding a nose boom and right- and left-wing-tip booms with Pitot-static heads and α- and β-vanes (not shown in fig. 1). The aircraft has a pulse-code modulation instrumentation system with telemetry as the only source of data. The measured data are recorded at the telemetry ground station. The instrumentation system includes transducers for the measurement of closed- and open-loop input variables, response variables, pressures on the prebody and quantities defining aircraft configuration, control system and engine operation, and instantaneous mass and inertia characteristics.

FLIGHT AND WIND TUNNEL DATA

The flight data of the tested aircraft were obtained from NASA Dryden Flight Research Facility in the form of time histories sampled at 50 samples/ sec. The measured data were corrected for the c.g. offset of the linear accelerometers, and α- and β-vanes. In addition, the α-vane readings were corrected for the upwash effect. The air data for the analysis were taken from the nose-boom sensors. From the data obtained, 33 longitudinal and 41 lateral maneuvers were analyzed. These maneuvers were initiated from mostly steady flights at altitudes between 5,000 and 9,500 m (17,000 and 31,000 ft) and an angle of attack between 8° and 54°. The pilot input for the longitudinal maneuvers was a pitch command in the form of a simple doublet. For the lateral responses, separate roll and yaw commands in the form of doublets were applied. Time histories of input and response variables from four maneuvers are presented in figures 2 to 5.

In figure 2 the longitudinal response of the aircraft at $\alpha \approx 8°$ is shown. The open-loop inputs included deflections of the horizontal tail, leading and trailing edge flaps. In this case, the short period motion of the aircraft seems to be well excited. Figure 3 shows an example of the longitudinal maneuver initiated at $\alpha \approx 44°$. Problems of insufficient excitation and maintaining uncoupled response are visible from the time histories of both the input and output variables. An example of lateral response of low angle of

2

attack is given in figure 4. The wide time separation of roll and yaw commands, and the short duration of the rudder doublet resulted in low information content of the measured data. Finally, the lateral maneuver initiated at $\alpha \approx 54°$ is presented in figure 5. The resulting responses exhibit strong coupling between the lateral and longitudinal motion and insufficient excitation of the lateral acceleration.

The estimated parameters from flight data were compared with the aerodynamic functions and parameters in the NASA LaRC flight simulator. These aerodynamic data are based on wind tunnel measurements with some adjustments for a previous flight test basis. The data are summarized in reference 1. The stability and control derivatives presented in this report were computed from aerodynamic functions for scheduled flap positions and horizontal tail deflections required to turn the aircraft at given flight conditions. The computed parameter C_{m_α} is referenced to the c.g. positions at 25 percent of the m.a.c.

FLIGHT DATA ANALYSIS

The first step in data analysis included a check on measured data compatibility and estimation of unknown bias errors in the measurement. Then the unknown parameters, in the form of stability and control derivatives, were estimated from postulated expressions for the aerodynamic coefficients. For the compatibility check the maximum likelihood method of reference 3 was applied. The state equations were represented by kinematic equations

$$\dot{x} = f(x, \eta, \Theta) \tag{1}$$

where

$$x = [u, v, w, \phi, \theta, \psi]^T$$

$$\eta = [a_x, a_y, a_z, p, q, r]^T$$

and Θ is a vector of unknown bias errors in measured input and response variables. The vector of response variables was formulated as

$$z = [V, \beta, \alpha, \phi, \theta, \psi]^T$$

Each measured response variable was expressed as

$$z_E = (1 + \lambda_z) z + b_z + n_z \tag{2}$$

where λ_z is the unknown scale factor error, b_z is the constant bias error and n_z is the measurement noise. For the measured inputs it was assumed that the scale factor errors and the measurement noise are equal to zero.

The unknown parameters and their Cramer-Rao bounds were obtained by minimizing the cost function

$$J = -\frac{1}{2} \sum_{i=1}^{N} v^T(i) R^{-1} v(i) - \frac{N}{2} \ln|R| \tag{3}$$

3

where

$$\nu(i) = z_E(i) - z(i,\hat{\theta})$$

R is the covariance matrix of measurement noise and N is the number of data points.

Estimates of aerodynamic parameters were obtained by using a stepwise regression method presented in reference 4. Because all the maneuvers exhibited small perturbations around initial conditions, the aerodynamic model equations were postulated with linear terms only. For the longitudinal maneuvers the regression model was formed as

$$C_a = C_{a_0} + C_{a_\alpha}\alpha + C_{a_q}\frac{q\bar{c}}{2V} + C_{a_{\delta H}}\delta_h \tag{4}$$

where a = Z and m, and for lateral maneuvers as

$$C_a = C_{a_0} + C_{a_\beta}\beta + C_{a_p}\frac{pb}{2V} + C_{a_r}\frac{rb}{2V} + C_{a_{\delta A}}\delta_a + C_{a_{\delta r}}\delta_r \tag{5}$$

where a = Y, ℓ and n.

In these equations the control effectiveness $C_{a_{\delta H}}$ includes the effect of the horizontal tail, as well as leading and trailing edge flaps deflection

$$C_{a_{\delta H}} = C_{a_{\delta h}} + \frac{\delta_f}{\delta_h}C_{a_{\delta f}} + \frac{\delta_{\ell f}}{\delta_h}C_{a_{\delta \ell f}} \tag{6}$$

and the control effectiveness $C_{a_{\delta A}}$ includes the effect of aileron, differential tail, and differential leading and trailing edge flaps deflection

$$C_{a_{\delta A}} = C_{a_{\delta a}} + \frac{\delta_{dh}}{\delta_a}C_{a_{\delta dh}} + \frac{\delta_{df}}{\delta_a}C_{a_{\delta df}} + \frac{\delta_{d\ell f}}{\delta_a}C_{a_{\delta \ell f}} \tag{7}$$

The regressors in (4) and (5) are represented by the increments of output and input variables from initial conditions. The unknown parameters are the stability and control derivatives and bias terms C_{a_0}. The dependent variables were computed from the following expressions:

$$C_Y = \frac{mg}{\bar{q}S} \, a_y$$

$$C_Z = \frac{mg}{\bar{q}S} \, a_z$$

$$C_\ell = \frac{I_X}{\bar{q}Sb} \left[\dot{p} - \left(\frac{I_Y - I_Z}{I_X}\right)qr - \frac{I_{XZ}}{I_X}(pq + \dot{r}) \right]$$

$$C_m = \frac{I_Y}{\bar{q}Sc} \left[\dot{q} - \left(\frac{I_Z - I_X}{I_Y}\right)pr - \frac{I_{XZ}}{I_Y}(r^2 + p^2) \right]$$

$$C_n = \frac{I_Z}{\bar{q}Sb} \left[\dot{r} - \left(\frac{I_X - I_Y}{I_Z}\right)pq - \frac{I_{XZ}}{I_Z}(\dot{p} - qr) \right]$$

In these equations, the angular accelerations were obtained by fitting cubic splines to measured angular velocities and then by differentiating the analytical expressions obtained.

The unknown parameters were obtained by minimizing the cost function

$$J = \sum_{i=1}^{N} \left[y(i) - \Theta_0 - \sum_{j=1}^{\ell} x_j(i)\Theta_j \right]^2 \qquad (8)$$

where y is the dependent variable, x_j are the regressors, and ℓ is the number of statistically significant terms in (4) and (5). The covariance matrix of the parameters was estimated as

$$\text{cov}(\hat{\Theta}) = s^2 (X^T X)^{-1} \qquad (9)$$

where X is the matrix of regressors and ones, and s^2 is the variance of the measurement noise.

RESULTS AND DISCUSSIONS

The results of flight data analysis are summarized in the following four sections. The first one contains a check on the compatibility between measured and predicted responses with the emphasis on air data accuracy. The second and third sections include estimates of longitudinal and lateral parameters and their comparison with wind tunnel measurement and flight results of reference 5. These results were obtained from several maneuvers using data partitioning and stepwise regression (see refs. 5 and 6). In the last section the effect of different input forms on the accuracy of estimated parameters is addressed.

5

Data Compatibility Check:

Two large amplitude maneuvers were used in the data compatibility check. The first maneuver consisted of slow deceleration with superimposed longitudinal transients. In the second maneuver, slow deceleration was combined with the lateral responses initiated by aileron and rudder deflections. The time histories of the output and input variables in this maneuver are shown in figure 6. Bias errors, their standard errors, and resulting fit errors estimated from the data of the first maneuver are presented in table II. The data were analyzed first by dividing the maneuver into three overlapping segments. Then, the data from the whole maneuver were used. The inconsistency among the four sets of estimates is probably caused by low excitation of transient motion and various amounts of information contained in each segment of the data. Small excitation of transient motion also resulted in strong pairwise correlations between parameters. These correlations degraded the accuracy of the estimates specified in table II.

Table III contains the results of estimation based on the data from the second maneuver. The approach to the analysis was similar to that used previously. This time, however, the postulated unknowns included constant biases in longitudinal and lateral variables, and scale factors λ_α and λ_β. The accuracy of the estimated scale factor λ_α was again degraded by strong correlation between b_α and λ_α. For that reason, it was not possible to verify the accuracy of upwash corrections applied to nose boom α-vane readings. The estimated values of λ_β indicate a possible change in the sidewash with the angle of attack.

For better evaluation of assumptions concerning the air data measurement, the time histories of residuals in the air speed, angle of attack, and sideslip angle were plotted in figure 7. These plots show a presence of uncorrected systematic errors which means that measurement equation (2) could not explain variations in measured air data. The same residuals are also plotted against the angle of attack in figure 8. From these plots a pronounced disagreement between measured and predicted angle of attack for $\alpha > 30°$ is seen. For further verification of air data accuracy the air speed and angle of attack are plotted in figure 9 against the corresponding variables V_L and α_L obtained from the left-wing-boom sensors. In the same figure the nose-boom sideslip angle was compared with the average value $\bar{\beta}$ obtained from both left- and right-wing-boom vanes. When calculating $\bar{\beta}$, no sidewash corrections were applied. From the plots in figure 9 it follows that $V > V_L$ in the whole range of α and there is a substantial discrepancy between α and α_L for $\alpha > 30°$. The similar plot of α against α_R from the right-wing boom exhibited the same pattern. This means that the upwash correction used in computing α is not correct for $\alpha > 30°$ and also that it needs some improvement for α from $10°$ to $18°$. Finally, there are differences between β and $\bar{\beta}$ which increase with increased sideslip angle. Assuming that

6

the sidewash corrections for the nose-boom β-vane are small (see results in table III) it can be concluded that the computed $\bar{\beta}$ is in error.

Because of low accuracy of estimated bias errors and the preliminary nature of the following results, no additional corrections to measured data were applied. For better assessment of the accuracy of measured responses more data from carefully designed experiments would have to be analyzed. In addition, the computing procedure for obtaining corrected values of V, β, and α should be revised and complemented by results from wind tunnel measurement of upwash and sidewash corrections.

Longitudinal Parameters:

The vertical-force and pitching-moment parameters are presented in figures 10 and 11. In these figures the variation of parameter estimates with the angle of attack, their consistency, and degree of agreement with wind tunnel measurement can be seen. The scatter in the most important parameters C_{Z_α}, C_{m_α}, and $C_{m_{\delta H}}$ is, in general, large and unacceptable for results of this research program. The consistency of the remaining parameters was expected to be low because of the low sensitivity and identifiability of these parameters. An improvement in parameter accuracy can be achieved by improving the accuracy of air data measurement and by selecting inputs which could improve the short-period excitation, especially at high angle-of-attack flight regimes.

The parameter estimates are in variable degrees of agreement with wind tunnel measurement. The main discrepancies are in C_{Z_α} for α between 13° and 22° and C_{m_α} for α between 10° and 20°. The estimated horizontal tail effectiveness, δ_H, is about 10 percent smaller than that from wind tunnel data. The wind tunnel values of C_{Z_q} are also substantially lower than the estimated values. The same applied for C_{m_q} for α between 20° to 40°.

Lateral Parameters:

The estimates of lateral parameters are presented in figures 12 to 16. The parameters expressing the sideslip effect are shown in figure 12. All three sets of these parameters exhibit large scatter, thus indicating poor accuracy of the estimates. The reason for this is insufficient excitation of lateral modes and uncorrected bias errors in measured sideslip angles. In addition, the values of C_{n_β} are low which further decreases the identifiability of this parameter. Because of large scatter in all three parameters it is difficult to assess their agreement with wind tunnel measurement or previous flight results. The exception is the parameter C_{Y_β}, whose values for α between 8° and 30° are closer to the estimates from reference 5 than to wind tunnel data.

7

The roll-rate and yaw-rate parameters are shown in figures 13 and 14. Good identifiability can be observed only in parameter C_{ℓ_p} for $\alpha < 23°$ and C_{Y_r} for $\alpha < 30°$. The values of these parameters at higher angles of attack and the estimates of the remaining dynamic parameters were found either inconsistent, statistically insignificant, or having nonphysical values. As in the previous case, the main reason for that is the small excitation of lateral modes.

The control parameters expressing the combined effect of the aileron, differential tail, and trailing edge flaps are plotted in figure 15. Large scatter and high values of $C_{\ell_{\delta A}}$ for $\alpha > 23°$ are caused by a near linear relationship between aileron and rudder deflections which can be seen in figures 4 and 5. As discussed in reference 7, near linear dependence among regressors, called data collinearity, results in inaccurate parameter estimates. The trend in the estimates in figure 15 indicates, however, that a new experiment which will decrease data collinearity and/or the use of biased estimation techniques introduced in reference 7 might result in estimates close to wind tunnel data. Similar conclusions can be made about the second set of control parameters expressing the effect of rudder deflection. These parameters are plotted in figure 16. Only the parameter $C_{Y_{\delta r}}$ was obtained with acceptable accuracy and good agreement with wind tunnel prediction.

Effect of Input Form on Parameter Estimates:

As indicated in the preceding sections, one way to improve the accuracy of estimated parameters is to select inputs which would sufficiently excite all modes included in the postulated model for the longitudinal and lateral motion of the aircraft. In order to demonstrate the effect of various input forms, the data from the flight simulator were recorded for two sets of inputs. The first set included repeats of pilot commands used in flight test. The second set contained the proposed inputs formed by a simple combination of doublets. Both sets of inputs and the pertinent response variables are shown in figures 17 to 20. The resulting parameters from the longitudinal data are given in table IV. This table includes estimated mean values, their standard errors, and increments of the multiple squared correlation coefficient. The last quantity mentioned indicates the amount of information in measured data explained by including individual terms into the regression equation representing the postulated aerodynamic model (see equations (4) and (5)). The selected input in figure 18, which combines three doublets in control stick deflection, substantially improves the accuracy of the estimates when compared with results where the input in the form of a single doublet was used. Also improved was the significance of the term C_{m_α} in the model as indicated by the corresponding values of ΔR^2. The difference in the estimated values of C_{m_α} is caused by the nonlinear form of the $C_m(\alpha)$ curve and by different amount of excitation in α. In both cases with different inputs the

8

parameter C_{z_q} was not identifiable, and the possibility of accurate estimation of C_{m_q} remains small.

The selected input in figure 20 for the excitation of the lateral motion combines rudder doublet immediately followed by the aileron doublet and then by a repeat of both doublets. This form of input excited the transient motion better than the input used in the flight test. The improvement in the information content of the data again reflected in improved accuracy of the parameters, especially of those expressing the sideslip effect, as shown in table V. In this table, only parameters of greater importance are included.

CONCLUDING REMARKS

Aerodynamic parameters of an advanced fighter aircraft were estimated from transient maneuvers at different angles of attack varying from 8 to 54 deg. For data analysis a stepwise regression with the ordinary least squares technique was applied. The resulting estimates were obtained in the form of aircraft stability and control derivatives. They were then presented as variations with the angle of attack and compared with wind tunnel measurement and a limited number of previous flight results. In addition to the analysis mentioned, the compatibility of measured data was checked and uncorrected bias errors in measured data estimated. The possible effect of various input forms on the accuracy of parameter estimates was demonstrated in two examples using simulated data. From all the results obtained the following conclusions can be drawn:

1. The existing maneuvers of data compatibility did not have enough information for accurate estimation of bias errors, especially for scale factor error in the α-vane readings. For that reason, no final statement about the accuracy of the measured data could be made.

2. Response variables in the longitudinal and lateral maneuvers for parameter estimation were, in general, not sufficiently excited. This was apparent mainly in low amplitudes of vertical acceleration, sideslip angle and yawing velocity, and also in some segments of lateral data where almost no transient motion occurred. Low excitation of response variables was caused by the selection of input forms and, in some cases, by difficulties in maneuvering the aircraft in the requested way.

3. Insufficient excitation of transient maneuvers resulted in large scatter in the estimated parameters and therefore in their low accuracy which is unacceptable for results of this research program.

4. The accuracy of lateral parameters was further degraded by near linear dependency between the aileron and rudder deflections.

9

5. Because of low accuracy of the parameter estimates it was not possible in many cases to comment on their agreement with wind tunnel measurement and previous flight data.

6. Simulated study showed that more careful selection of input forms can significantly improve the identifiability of the main parameters in the model.

The future experiment of obtaining accurate parameter estimates should include the following:

1. Special maneuver designed for the assessment of data compatibility.

2. Selection of input forms for an adequate excitation of transient maneuvers for parameter estimation. These inputs must be acceptable to the pilot and verified in the simulator.

3. Excitation of longitudinal and lateral maneuvers at different values of the angle of attack covering the range from approximately 8° to 50°.

4. Repeat of maneuvers at two or three selected values of the angle of attack for better assessment of parameter accuracy.

REFERENCES

1. Anon: "F/A-18 Stability and Control Data Report," Vol. I and II, MDC A7247, McDonnell Aircraft Company, 1982.

2. Anon: "F/A-18 Flight Control System Design Report," Vol. I and II, MDC A7813, McDonnell Aircraft Company, 1982.

3. Klein, Vladislav; and Morgan, Dan R.: "Estimation of Bias Errors in Measured Airplane Responses Using Maximum Likelihood Methods," NASA TM-89059, 1987.

4. Klein, Vladislav; Batterson, James G.; and Murphy, Patrick C.: "Determination of Airplane Model Structure From Flight Data by Using Modified Stepwise Regression," NASA TP-1916, 1981.

5. Hess, Robert A.: "Subsonic F/A-18A and F/A-18B (TF-18A) Aerodynamic Identified From Flight Test Data," System Control Technology (Patuxent River Office), Report No. 4522-220-1, 1987.

6. Batterson, James G.; and Klein, Vladislav: "Partitioning of Flight Data For Aerodynamic Modeling of Aircraft at High Angles of Attack," Journal of Aircraft, Vol. 26, No. 3, April 1989, pp.   .

7. Klein, Vladislav: "Two Biased Estimation Techniques in Linear Regression. Application to Aircraft," NASA TM-100649, 1988.

Table I. Geometric, Mass and Inertia Characteristics
of Aircraft.

Total length, m   17.07

Wing:
    Area, m^2 37.16
    Span, m   11.41
    Mean geometric chord, m   3.51
    Aspect ratio   3.5
    Quarter-chord sweep angle, deg   20.0

Horizontal tail:
    Area (wetted), m^2 16.35
    Span, m   6.58
    Mean geometric chord, m   1.91
    Aspect ratio   2.4
    Quarter-chord sweep angle, deg   42.8
    Moment arm (c.g. at 0.25 m.a.c.), m   5.12

Vertical tail:
    Area (wetted), m^2 9.66
    Mean geometric chord, m   2.13
    Aspect ratio   1.2
    Quarter-chord sweep angle, deg   35.0
    Cant, deg   20.0
    Moment arm (c.g. at 0.25 m.a.c.), m   3.10

Mass, kg   14,400

Inertia:
    I_X, kg-m^2 28,880
    I_Y, kg-m^2 165,930
    I_Z, kg-m^2 185,030
    I_{XZ}, kg-m^2 − 2,630

Table II. Estimates of Bias and Fit Errors From
Longitudinal Maneuver.

Parameter	Segment of data analyzed			
	0<t<40 sec 0<α<32 deg	20<t<60 sec 18<α<37 deg	39<t<79 sec 23<α<46 deg	10<t<70 sec 12<α<46 deg
b_V, m/sec	− .84 (.023)	− .32 (.020)	.20 (.060)	.03 (.047)
b_α, deg	.02 * (.022)	.61 * (.040)	− 2.3 * (.11)	.55 * (.095)
λ_α	− .020 * (.0026)	− .040 * (.0016)	.051 * (.0031)	− .034 * (.0053)
b_q, deg/sec	− .0159 * (.00013)	.0191 * (.0012)	.0146 * (.00074)	− .0220 * (.00013)
b_θ, deg	− .127 * (.0030)	.098 * (.0027)	.38 * (.017)	− .050 * (.0046)
b_{ax}, g units	.0046 (.00017)	.0036 (.00010)	.0208 (.00037)	.0060 (.00027)
b_{az}, g units	.0069 * (.00027)	.00718 (.000088)	.0041 (.00023)	.0053 * (.00039)
s(V), m/sec	.508	.448	1.281	.874
s(α), deg	.139	.176	.726	.634
s(θ), deg	.069	.061	.393	.089

Numbers in the parenthesis are standard errors
*) Parameter with strong correlation

Table III. Estimates of Bias and Fit Errors From
Lateral Maneuver.

Parameter	Segment of data analyzed			
	0<t<30 sec 9<α<27 deg	15<t<45 sec 14<α<41 deg	29<t<59 sec 24<α<47 deg	10<t<47 sec 11<α<47 deg
b_v, m/sec	.13 (.093)	.33 (.033)	1.52 (.071)	2.48 (.070)
b_α, deg	.2 * (.16)	.86 * (.036)	- 3.9 * (.14)	.20 * (.053)
λ_α	- .02 * (.021)	- .056 * (.0025)	.108 * (.0046)	- .138 * (.0031)
b_β, deg	.29 (.096)	- .104 (.0083)	.23 (.018)	.13 (.015)
λ_β	.04 (.10)	- .008 (.0035)	- .090 (.0018)	- .091 (.0036)
b_p, deg/sec	.025 (.0039)	.0051 * (.00064)	.007 * (.0011)	.0083 * (.00056)
b_q, deg/sec	.0127 * (.00078)	.0165 * (.00030)	.0482 * (.00049)	.0083 * (.00031)
b_r, deg/sec	.147 (.0040)	.1276 (.00024)	.105 * (.0010)	.1218 (.00034)
b_ϕ , deg	- .03 (.065)	.01 (.012)	- .44 (.016)	- .232 (.017)
b_θ, deg	- .05 * (.013)	.040 * (.0051)	.109 * (.0082)	.176 * (.0082)
b_{ax}, g units	.0112 (.00090)	.0189 (.00027)	.0388 (.00037)	.0290 (.00032)
b_{ay}, g units	.017 (.0019)	- .0069 * (.00020)	- .0044 * (.00040)	- .0041 * (.00024)
b_{az}, g units	.009 * (.0023)	.0084 * (.00038)	.010 * (.0015)	.0126 (.00027)

Numbers in parenthesis are standard errors
*) Parameters with strong correlation

Table III. Concluded.

Parameter	Segment of data analyzed			
	0<t<30 sec 9<α<27 deg	15<t<45 sec 14<α<41 deg	29<t<59 sec 24<α<47 deg	10<t<47 sec 11<α<47 deg
$s(V)$, m/sec	.182	.569	1.442	1.293
$s(\alpha)$, deg	.102	.159	.873	.665
$s(\beta)$, deg	.115	.154	.339	.236
$s(\phi)$, deg	.186	.265	.461	.367
$s(\theta)$, deg	.042	.097	.158	.140
$s(\psi)$, deg	.095	.174	.340	.336

Table IV. Estimates of Parameters From Two Longitudinal
Maneuvers With Different Input Forms.

Parameter	Flight input			Selected input		
	$\hat{\theta}$	$s(\hat{\theta})$	ΔR^2 [%]	$\hat{\theta}$	$s(\hat{\theta})$	ΔR^2 [%]
C_{z_α}	− 5.3	.22	64.9	− 5.52	.062	93.0
$C_{z_{\delta H}}$	− .97	.097	5.4	− .88	.063	1.6
C_{m_α}	− .20	.075	.3	− .43	.022	3.3
C_{m_q}	− 9.	2.3	.9	− 4.1	.98	1.1
$C_{m_{\delta H}}$	− 1.42	.034	81.5	− 1.35	.022	87.3

Table V. Estimates of Parameters From Two Lateral
Maneuvers With Different Input Forms

Parameter	Flight input			Selected input		
	$\hat{\Theta}$	$s(\hat{\Theta})$	ΔR^2 [%]	$\hat{\Theta}$	$s(\hat{\Theta})$	ΔR^2 [%]
C_{Y_β}	− 1.11	.041	14.2	− 1.11	.0076	70.5
$C_{Y_{\delta r}}$	.209	.0047	69.2	.245	.0024	27.6
C_{ℓ_β}	− .124	.0041	5.0	− .123	.00076	14.3
C_{ℓ_p}	− .411	.0085	5.5	− .418	.0042	6.8
$C_{\ell_{\delta A}}$	− .121	.0010	87.8	− .113	.00059	74.6
C_{n_β}	.13	.027	1.7	.131	.0049	15.8
C_{n_r}	− .2	.24	.1	− .14	.069	.1
$C_{n_{\delta r}}$	− .081	.0031	51.3	− .081	.0015	70.1

17.06 m
(56.0 ft.)

4.66 m
(15.3 ft.)

11.43 m
(37.5 ft.)
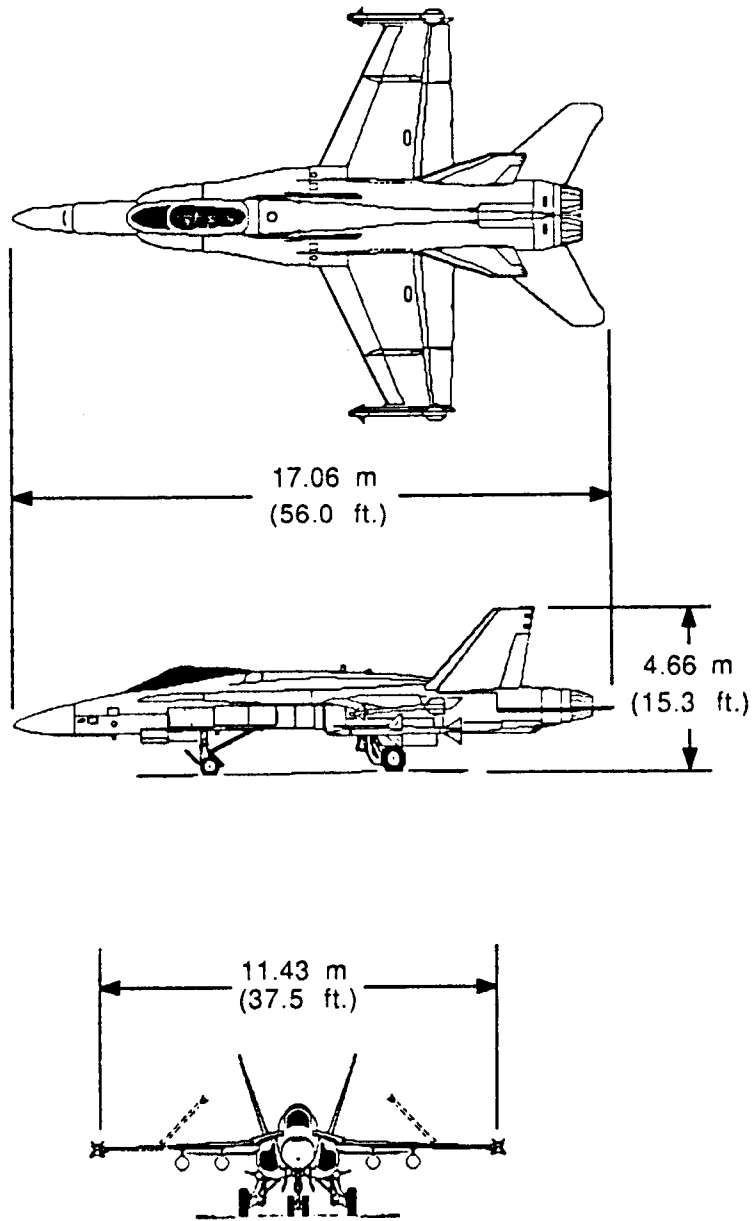
Figure 1.   Three-view drawing of test aircraft.
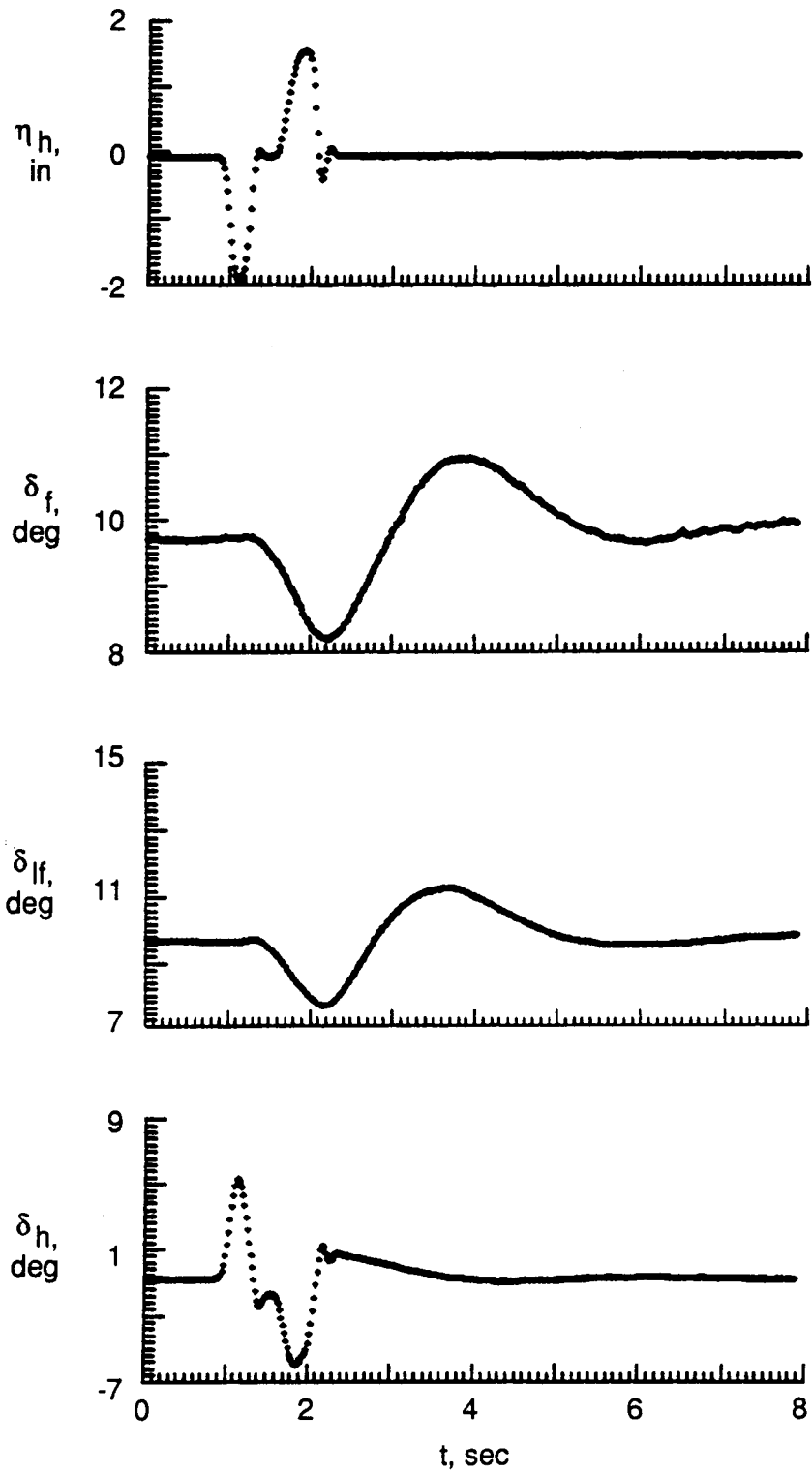
Figure 2. Time histories of measured input and response
variables in longitudinal maneuver ($\alpha_0 \approx 8°$).

19
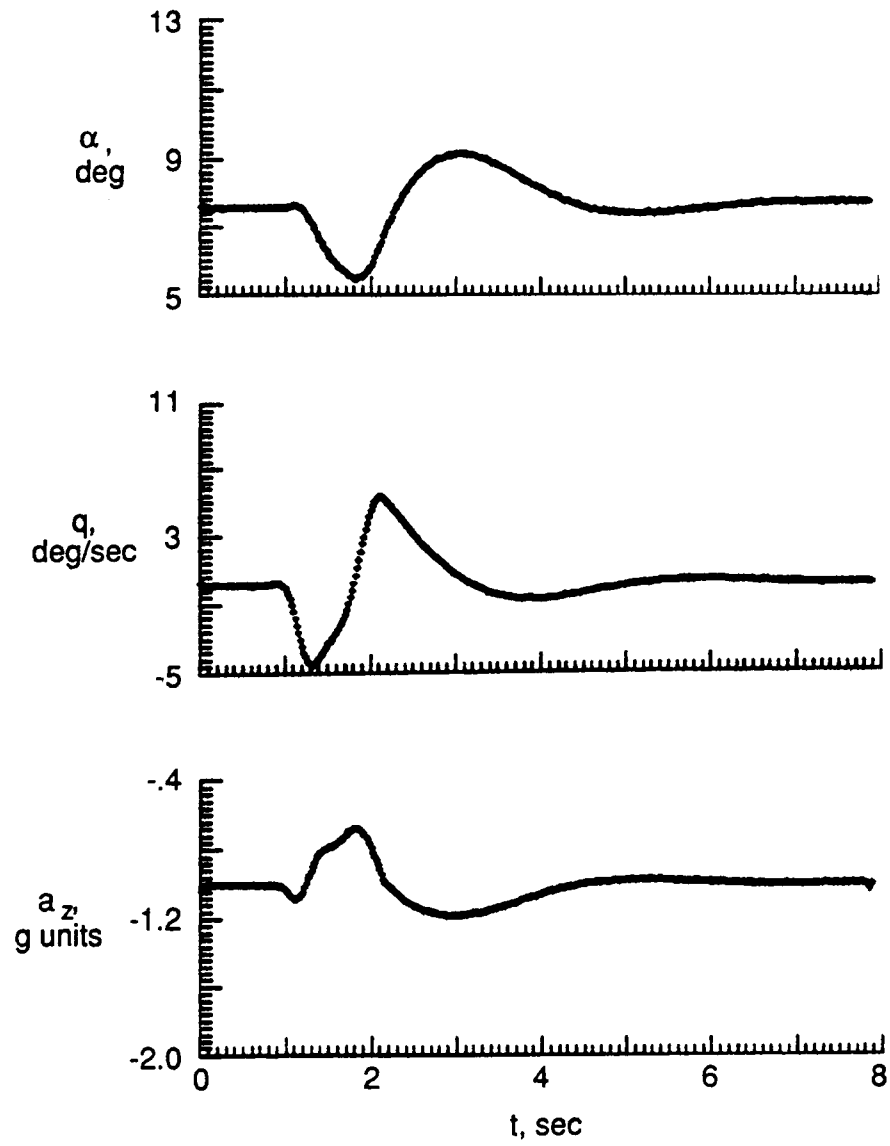
Figure 2.   Concluded

20
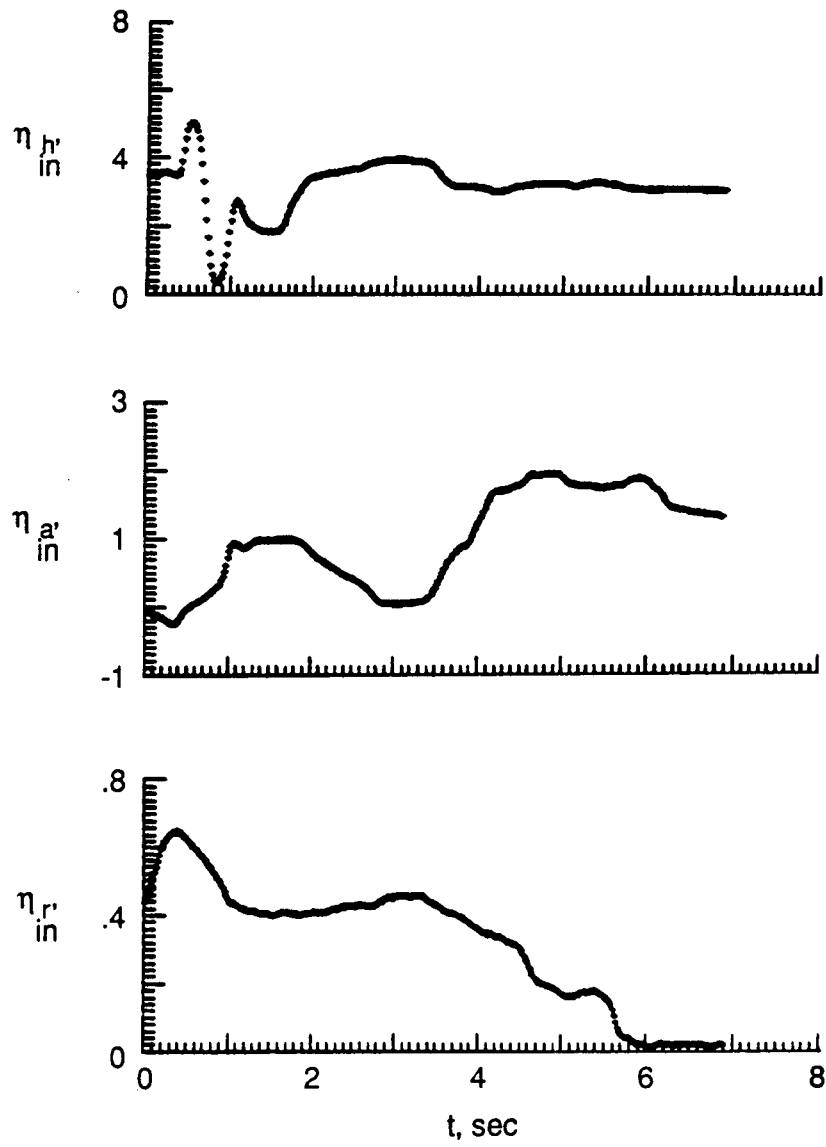
Figure 3. Time histories of measured input and response
variables in longitudinal maneuver ($\alpha_0 \approx 44^\circ$).

21

Figure 3. Continued

22

Figure 3. Continued

23
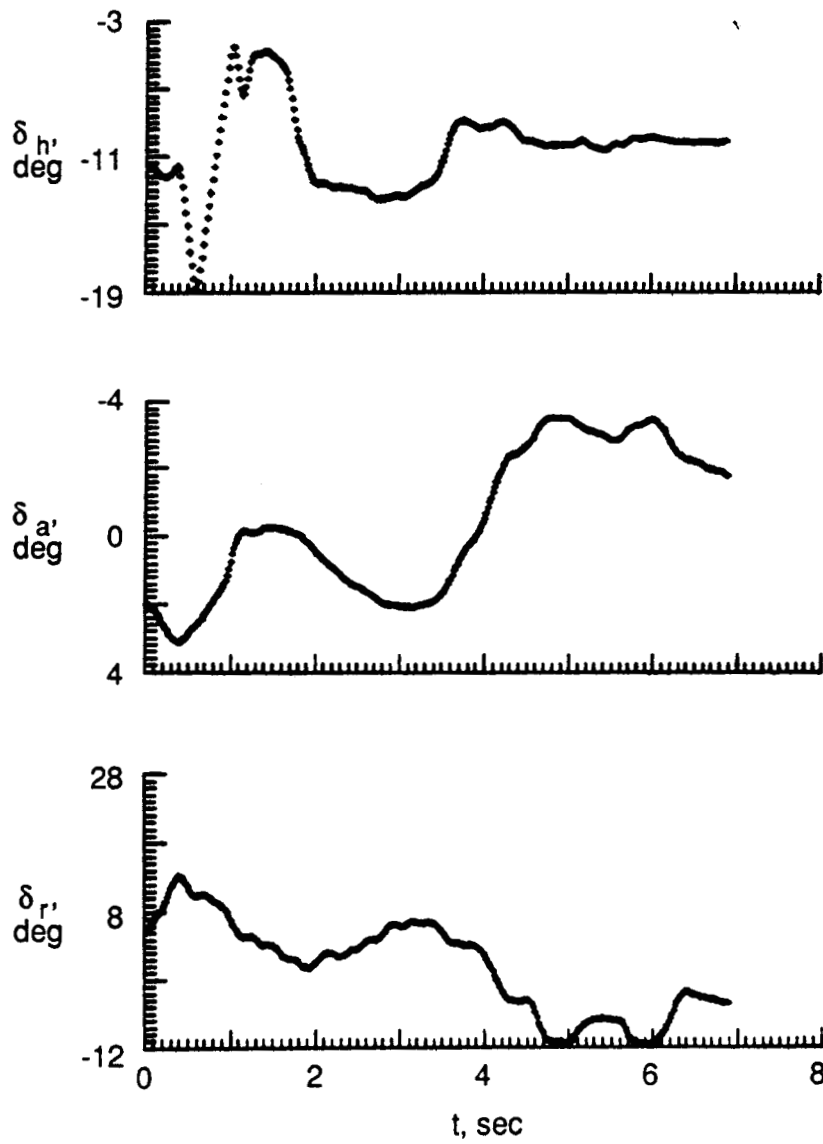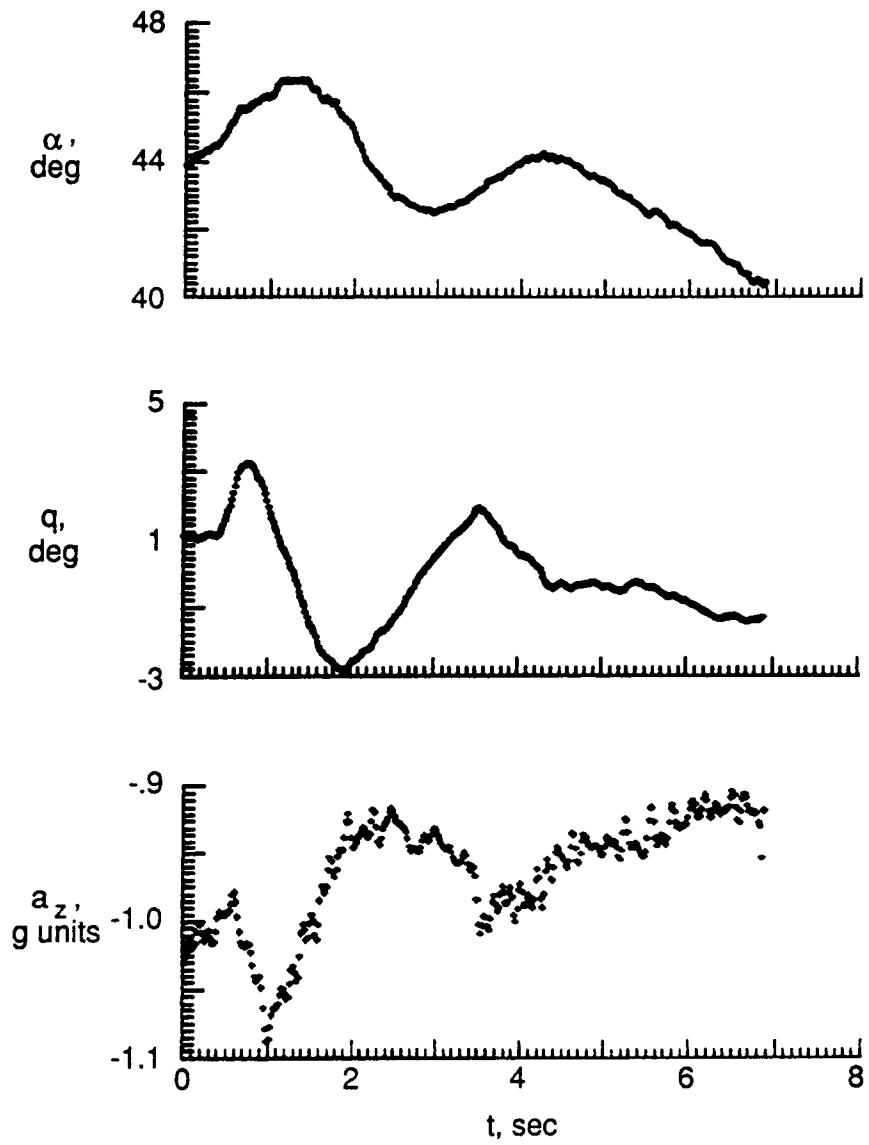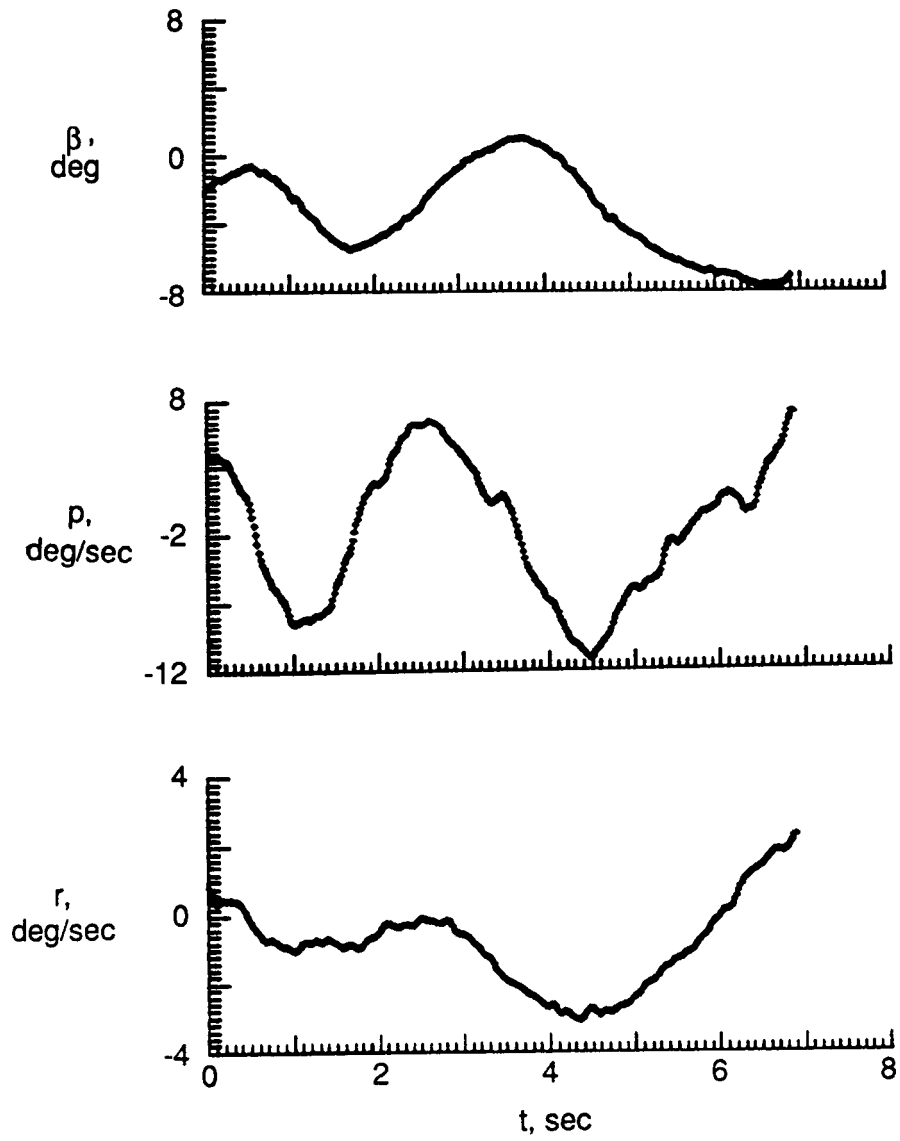
Figure 3.   Concluded

24
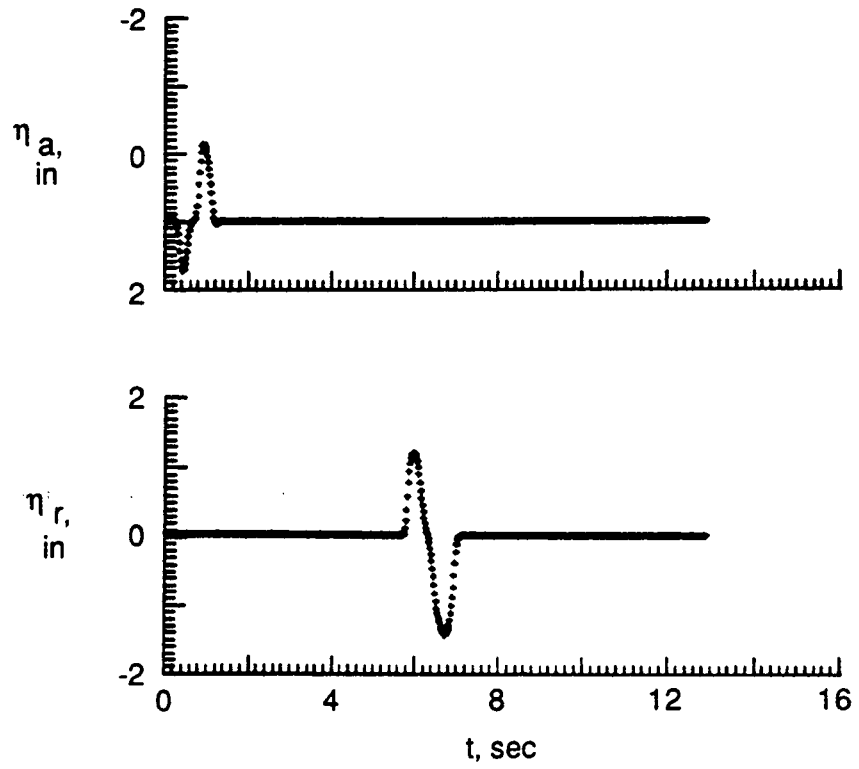
Figure 4. Time histories of measured input and response
variables in lateral maneuver ($\alpha_0 \approx 11^\circ$).

Figured 4. Continued

26
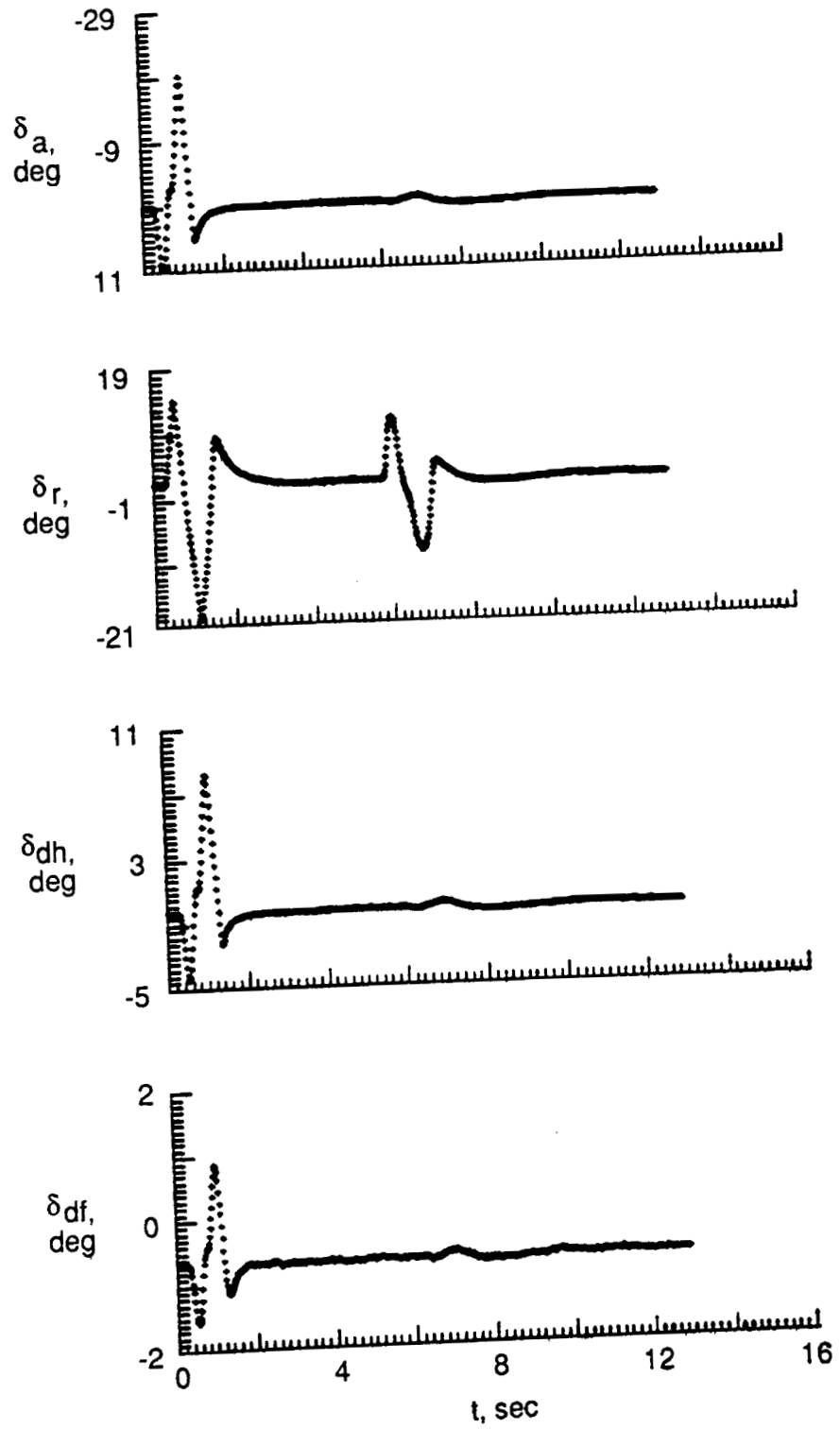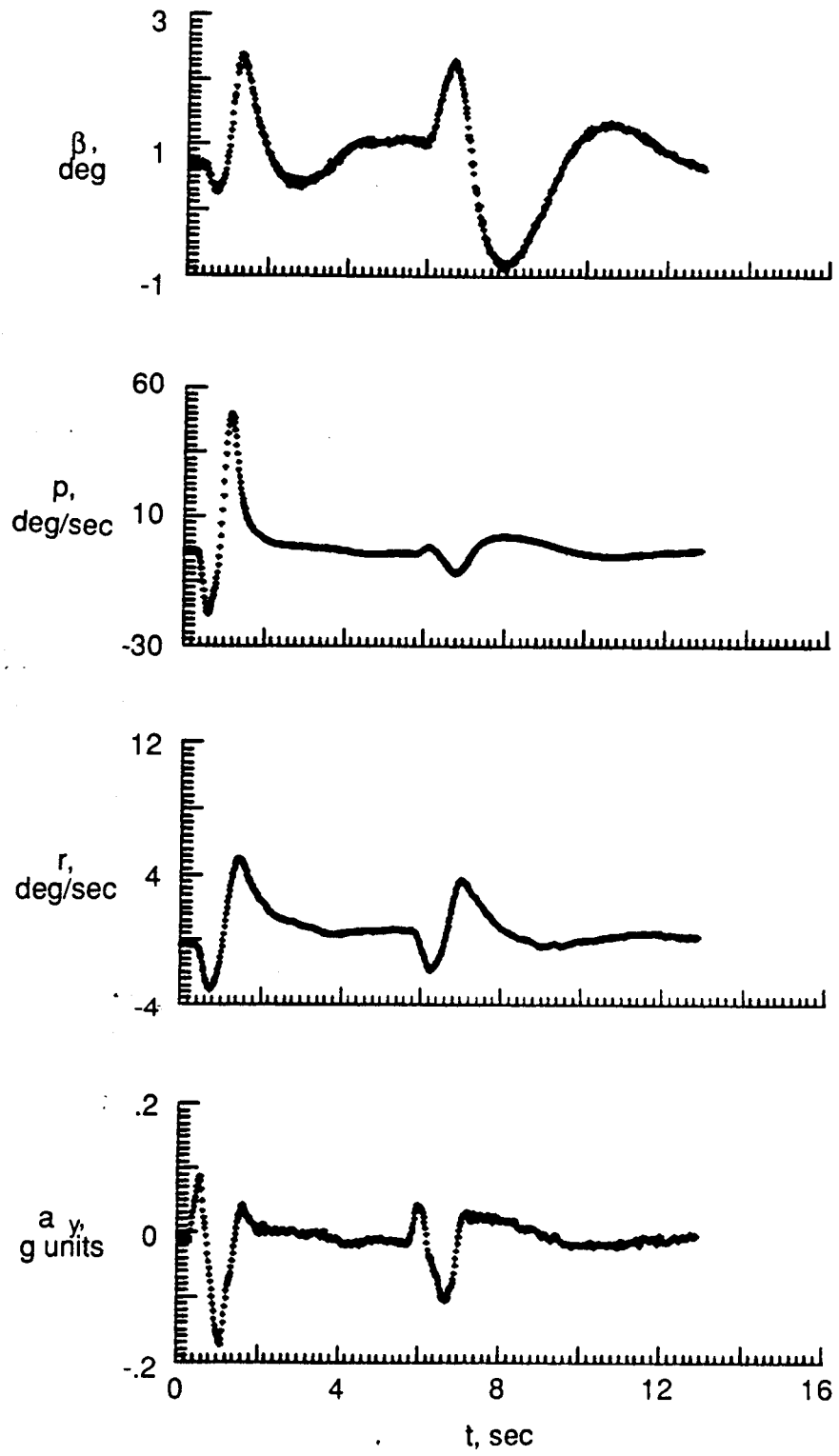
Figure 4. Concluded

27
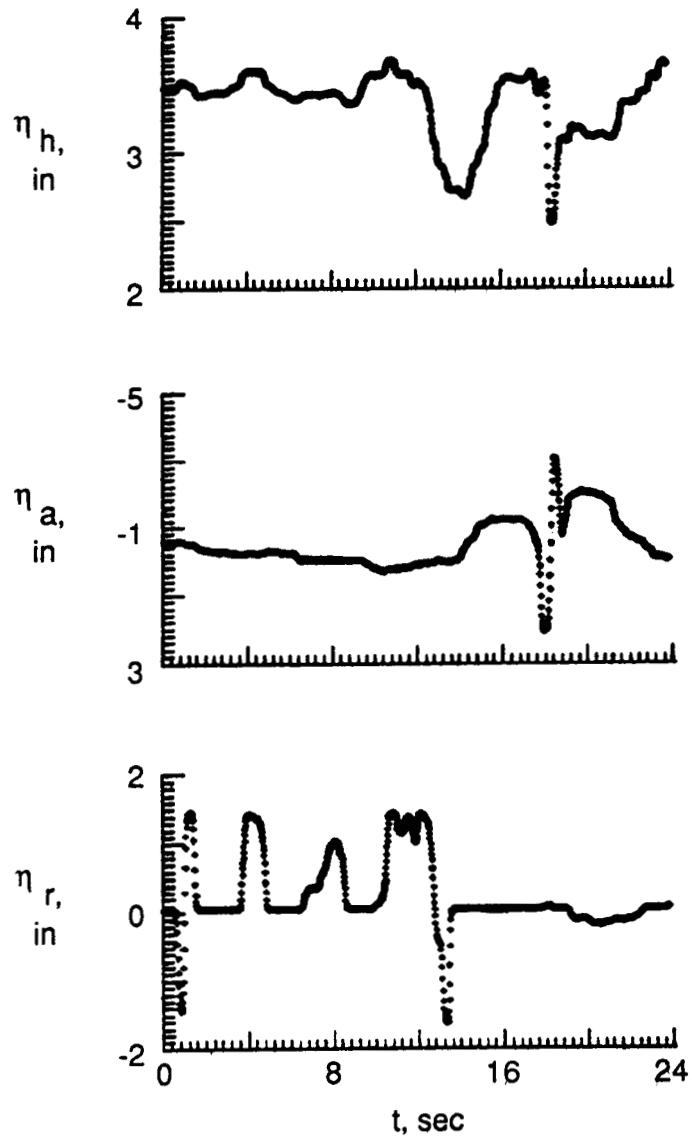
Figure 5. Time histories of measured input and response variables in lateral maneuver ($\alpha_0 \approx 54°$).
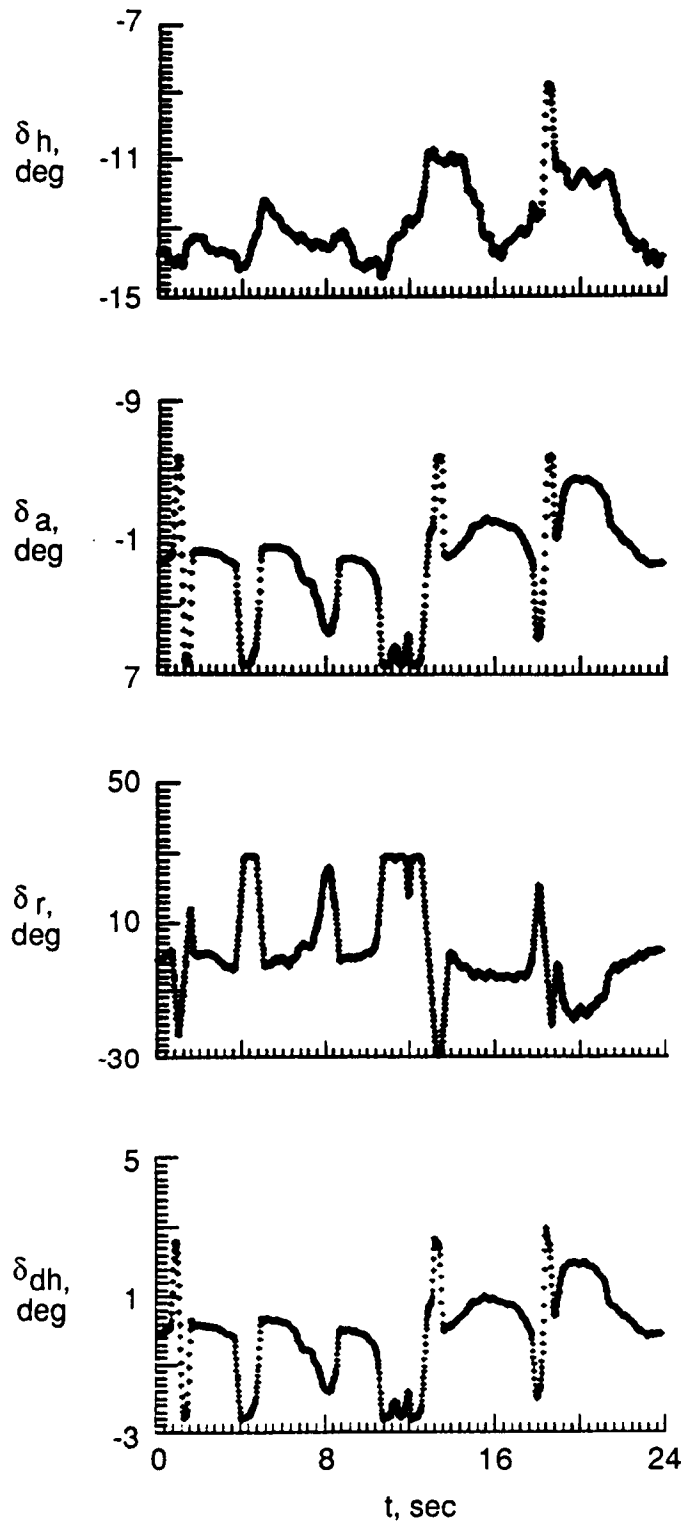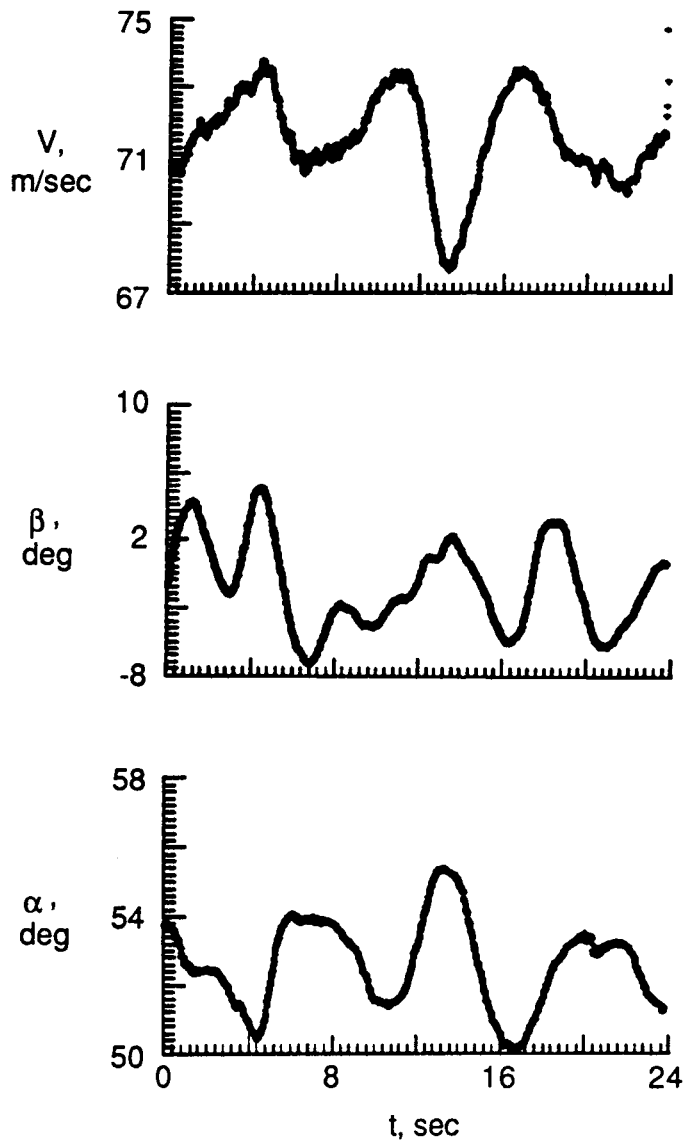
Figure 5. Continued

Figure 5.   Continued

30
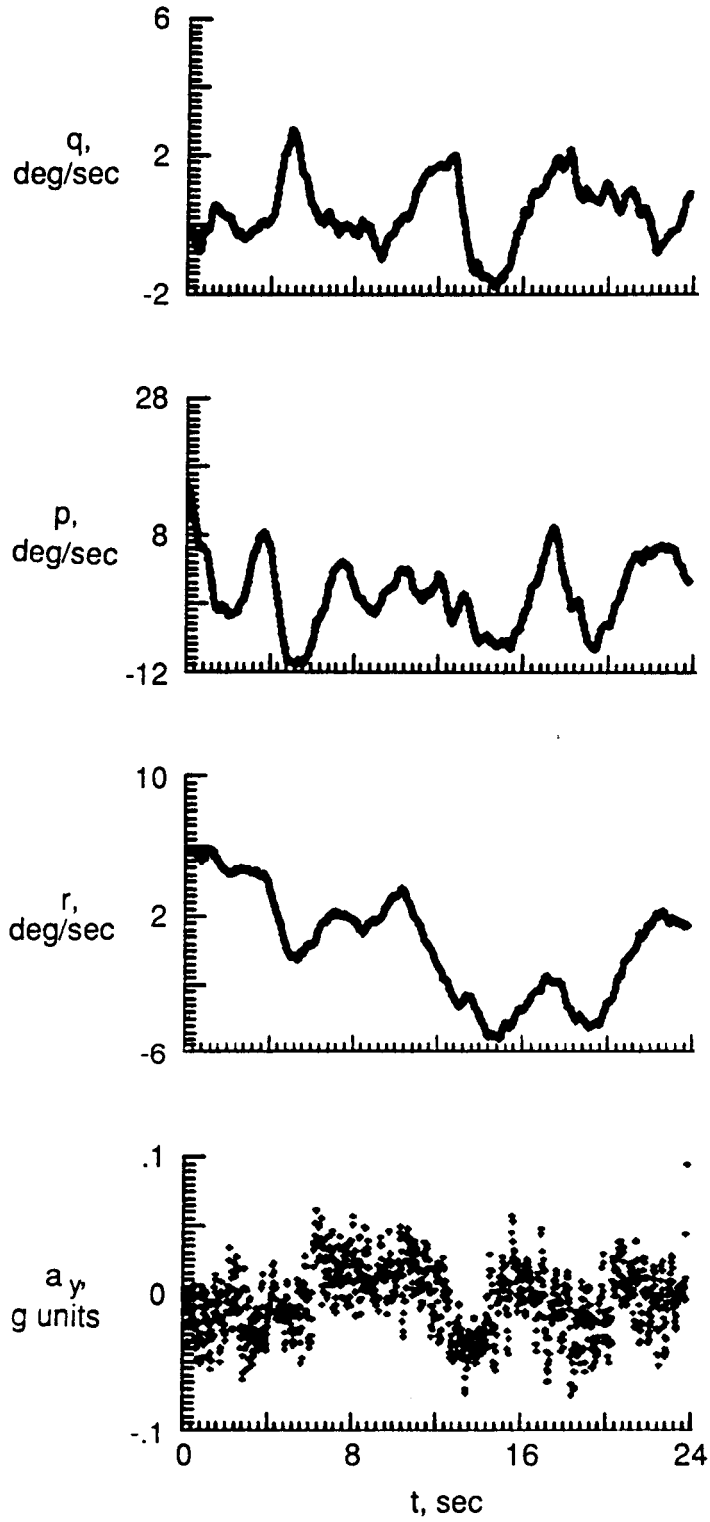
Figure 5. Concluded
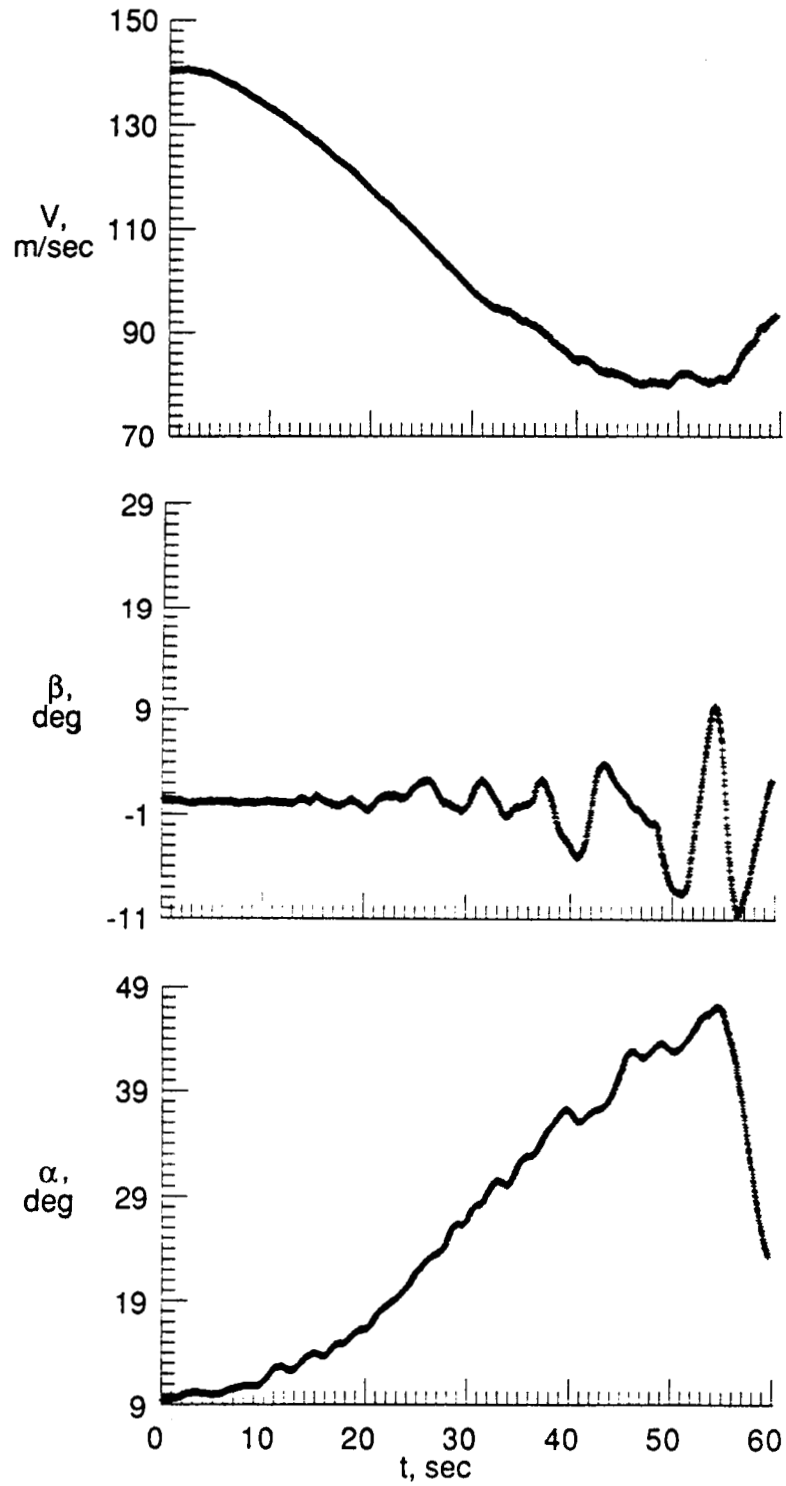
Figure 6. Time histories of measured response variables in large amplitude longitudinal maneuver.

Figure 6.   Continued

33

Figure 6.   Continued

34
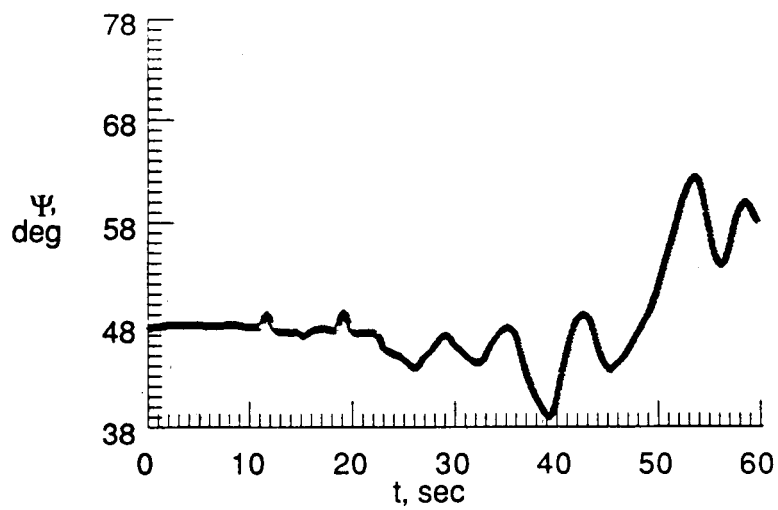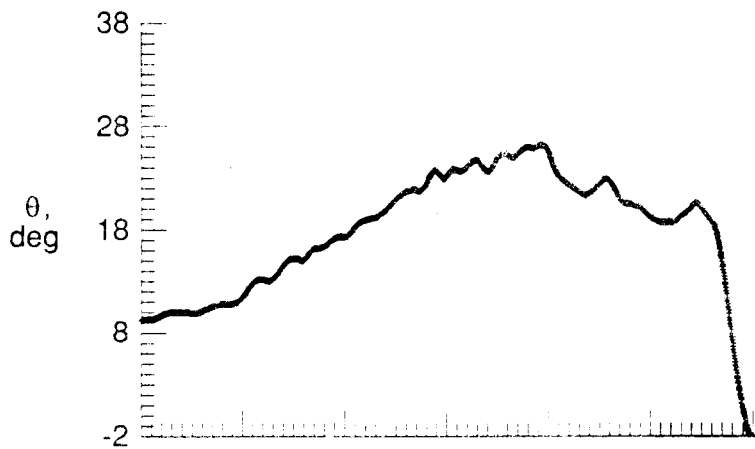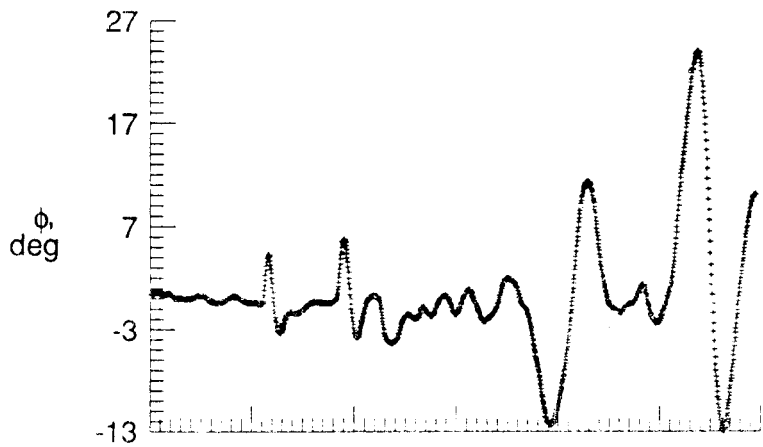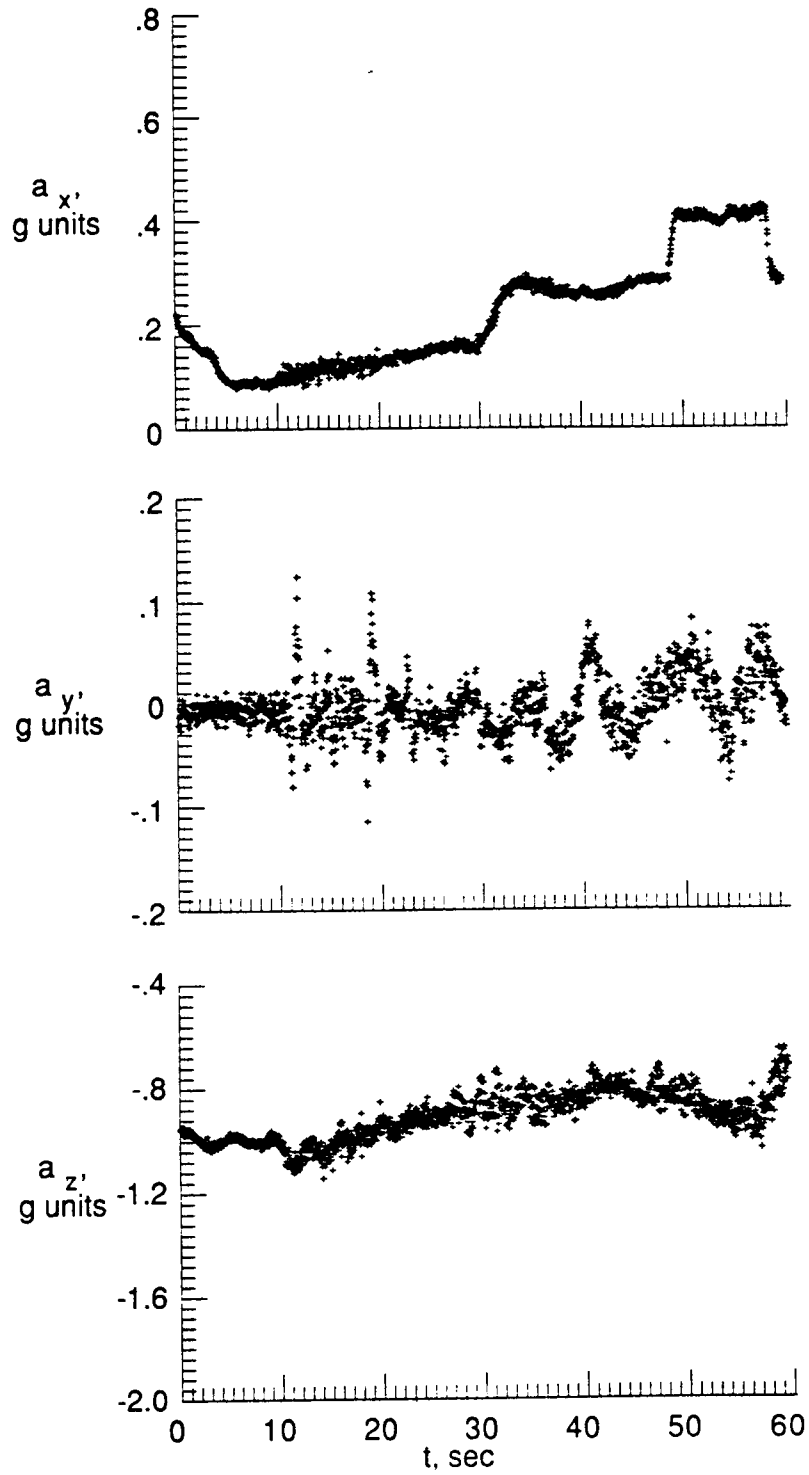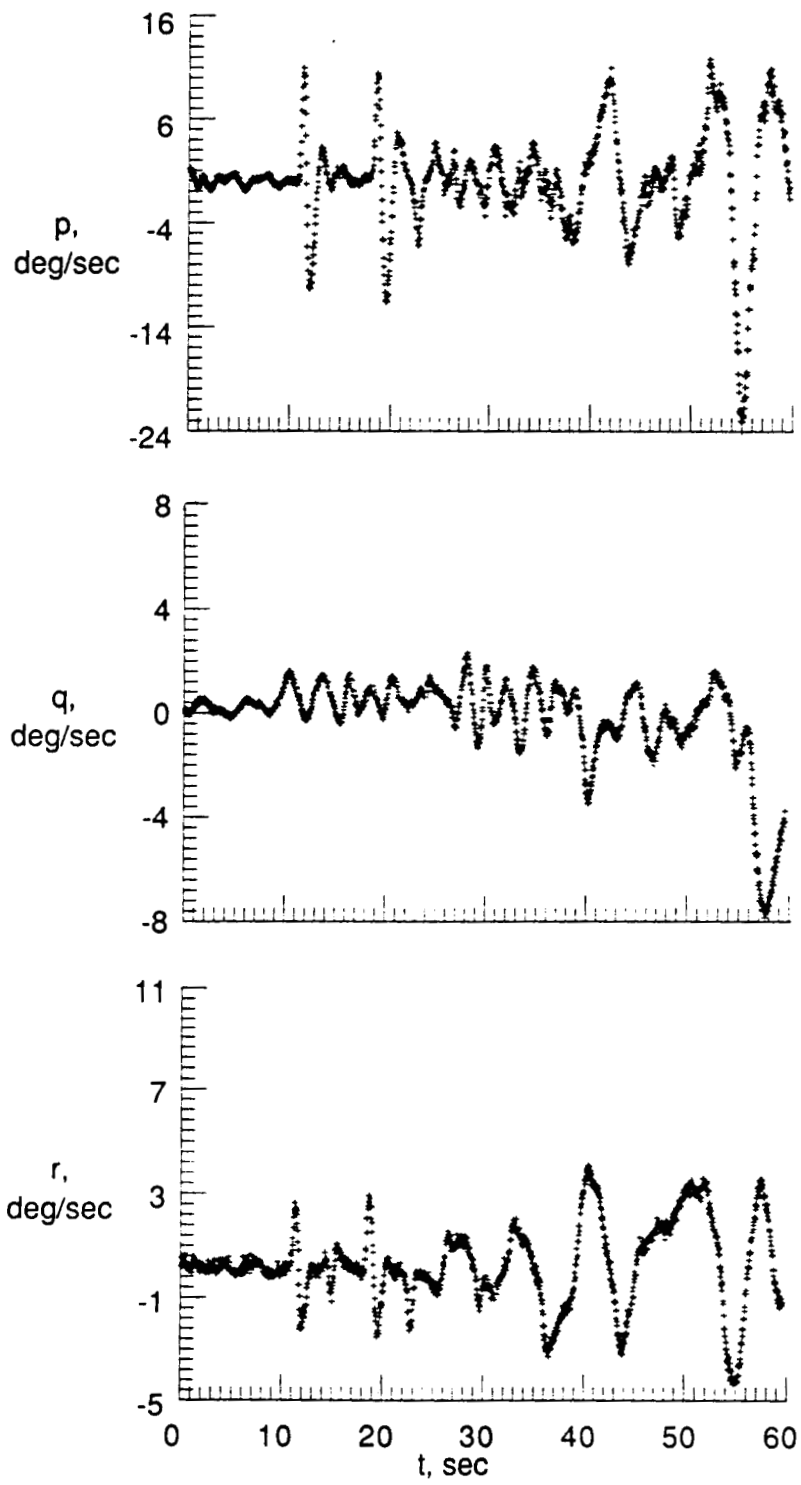
Figure 6. Concluded

35
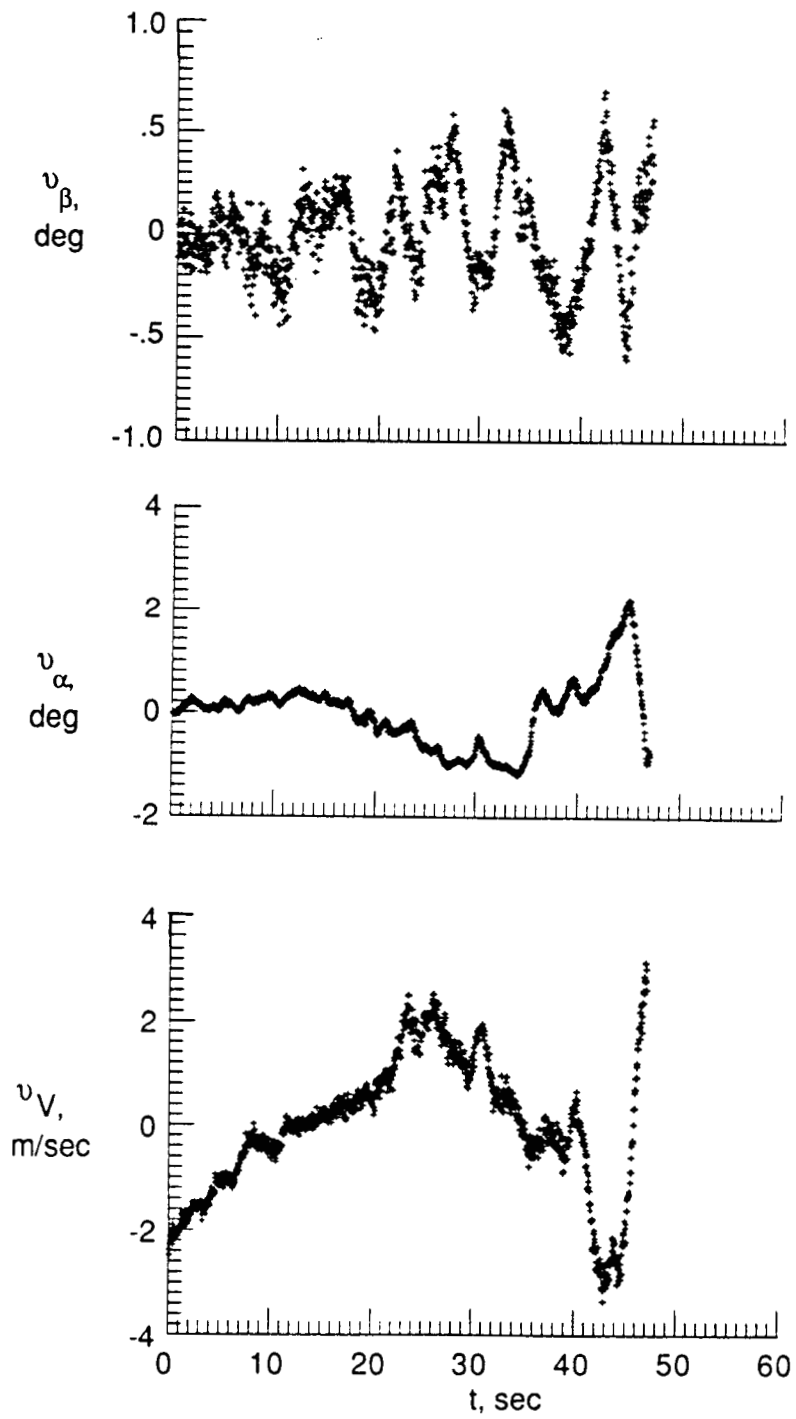
Figure 7.   Time histories of residuals.
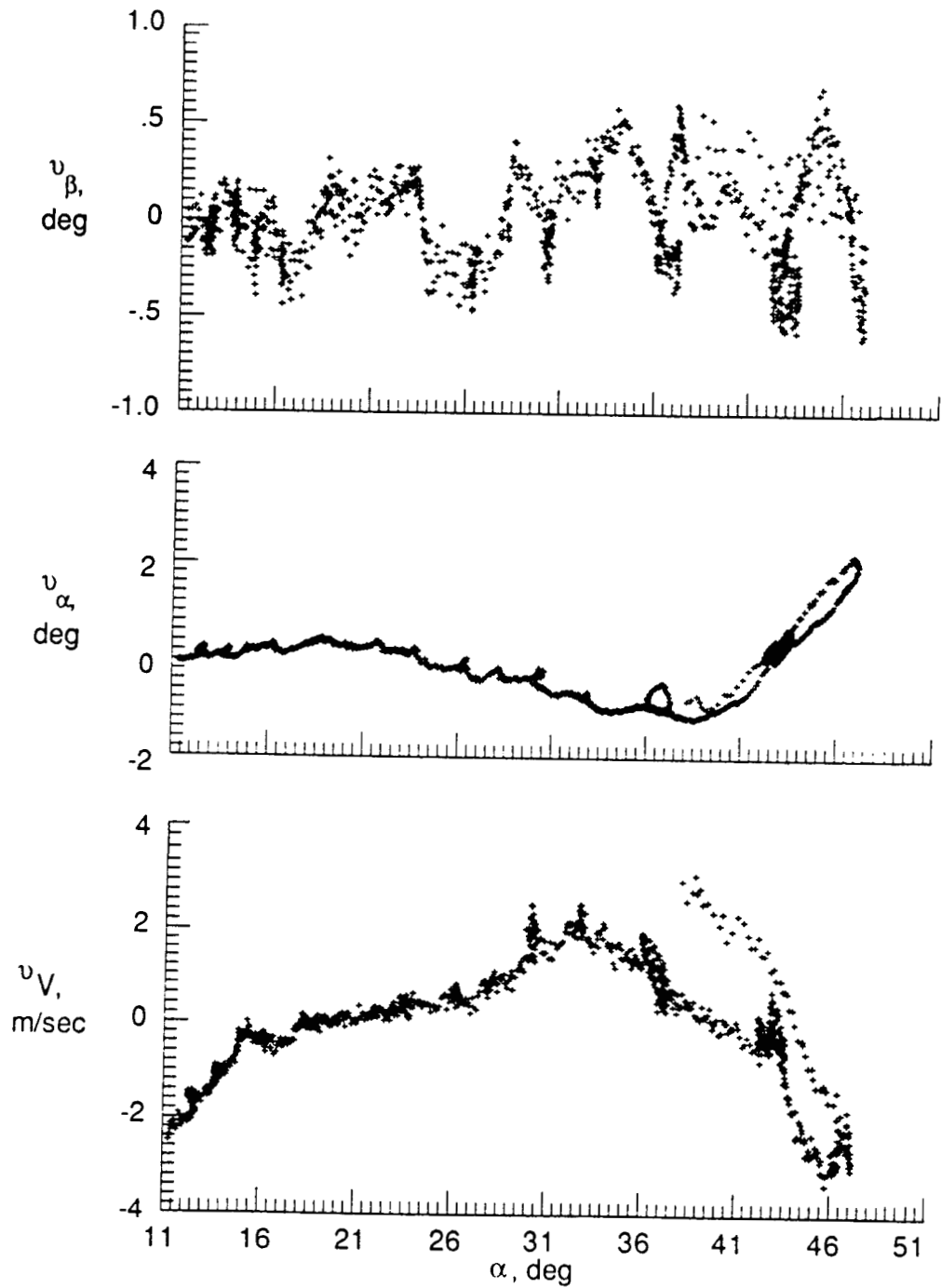
Figure 8.   Variation of residuals with angle-of-attack.
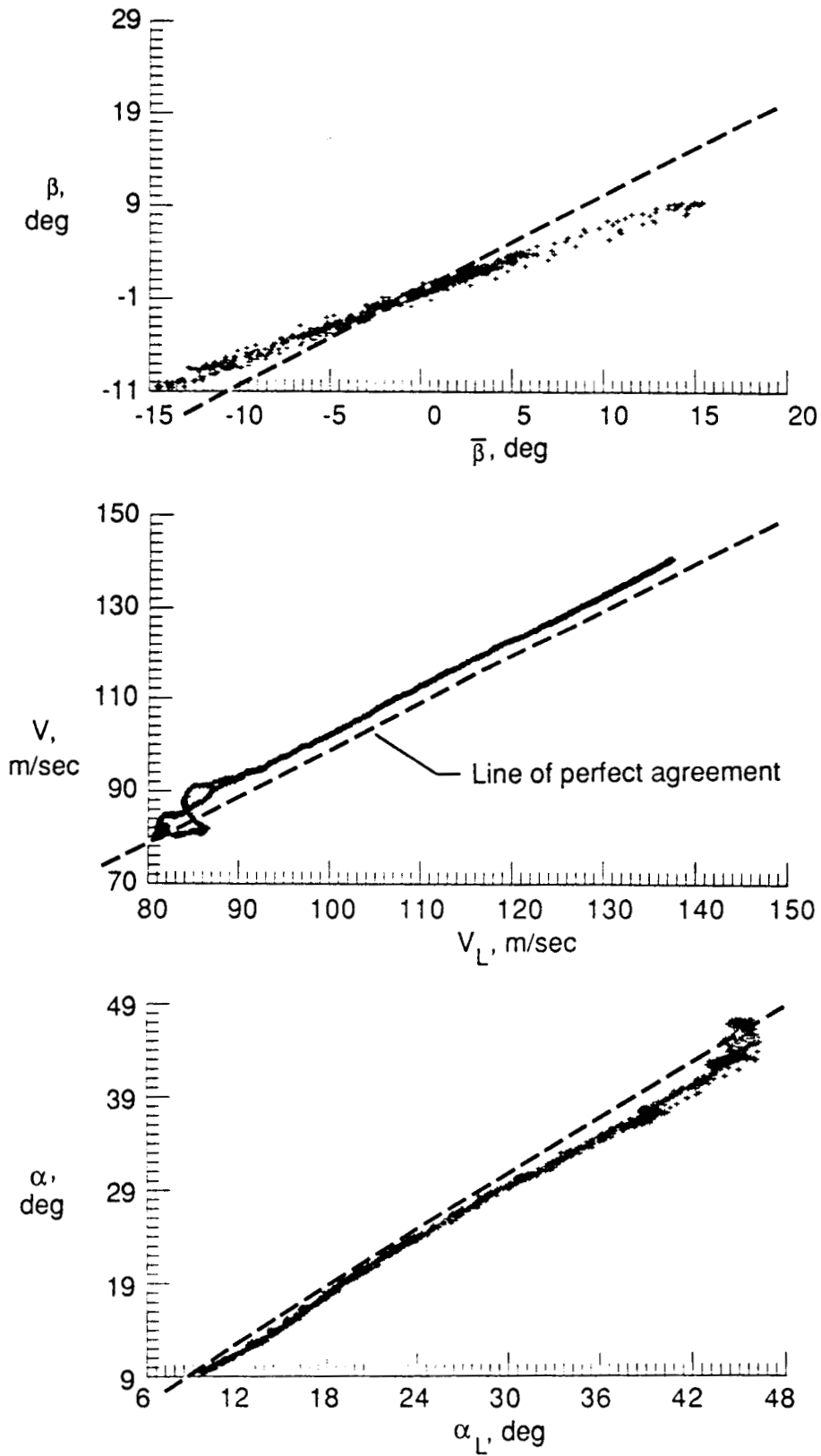
Figure 9.   Relationship between air data from nose boom
and left wing boom.
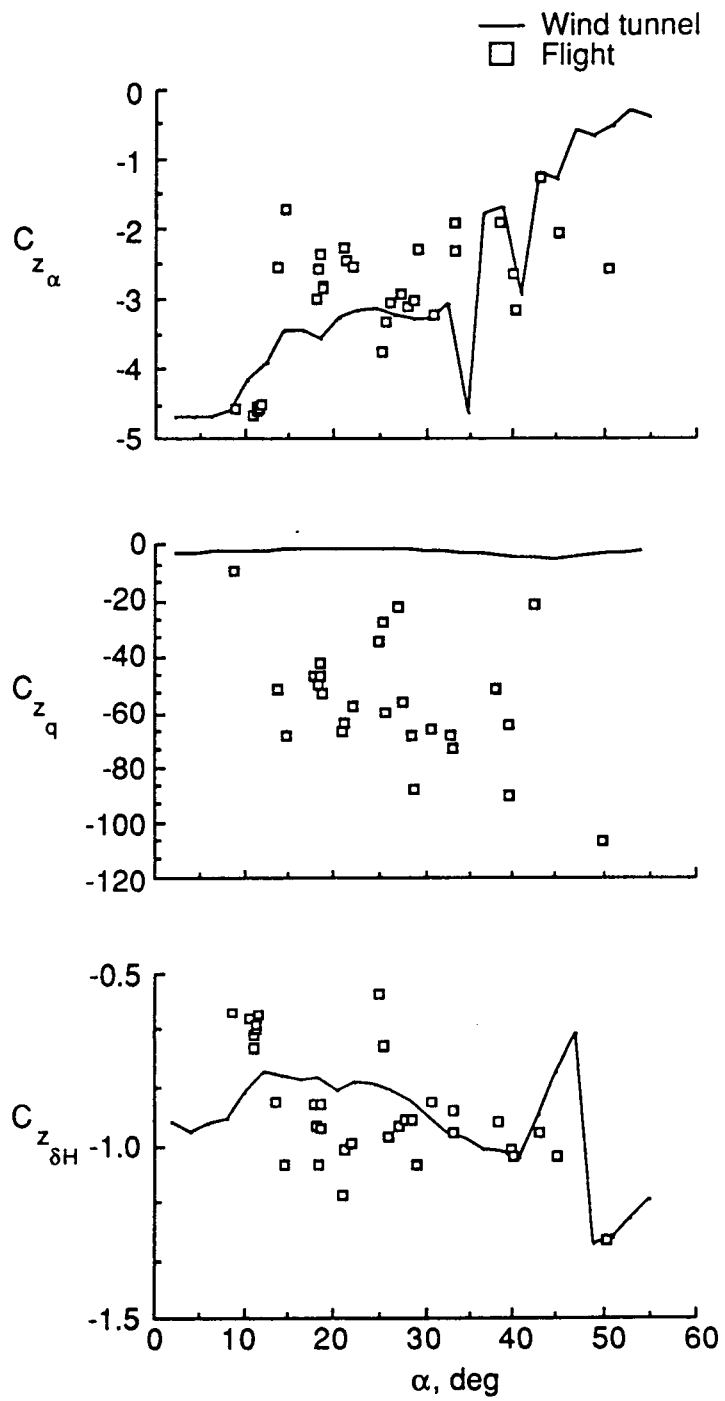
Figure 10. Comparison of vertical-force parameters
obtained from flight and wind tunnel
measurement.
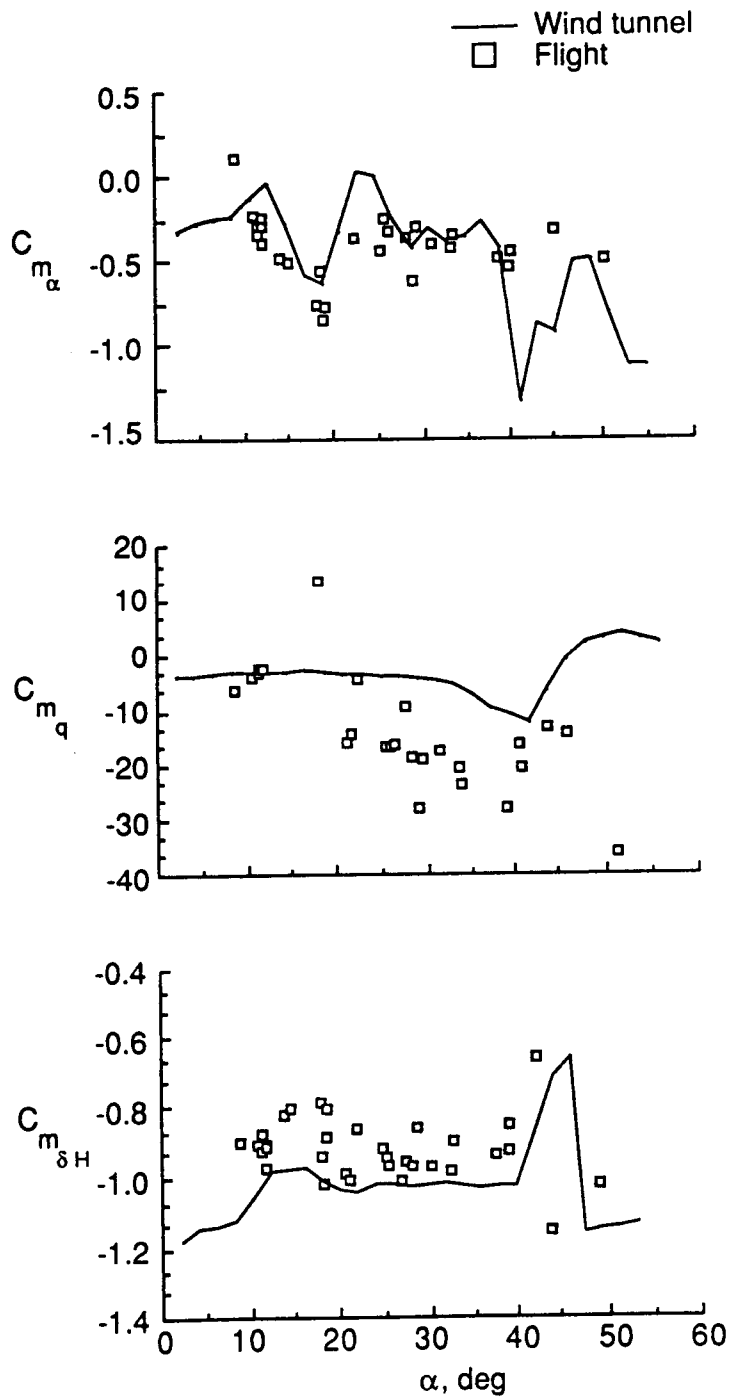
Figure 11.   Comparison of pitching-moment parameters
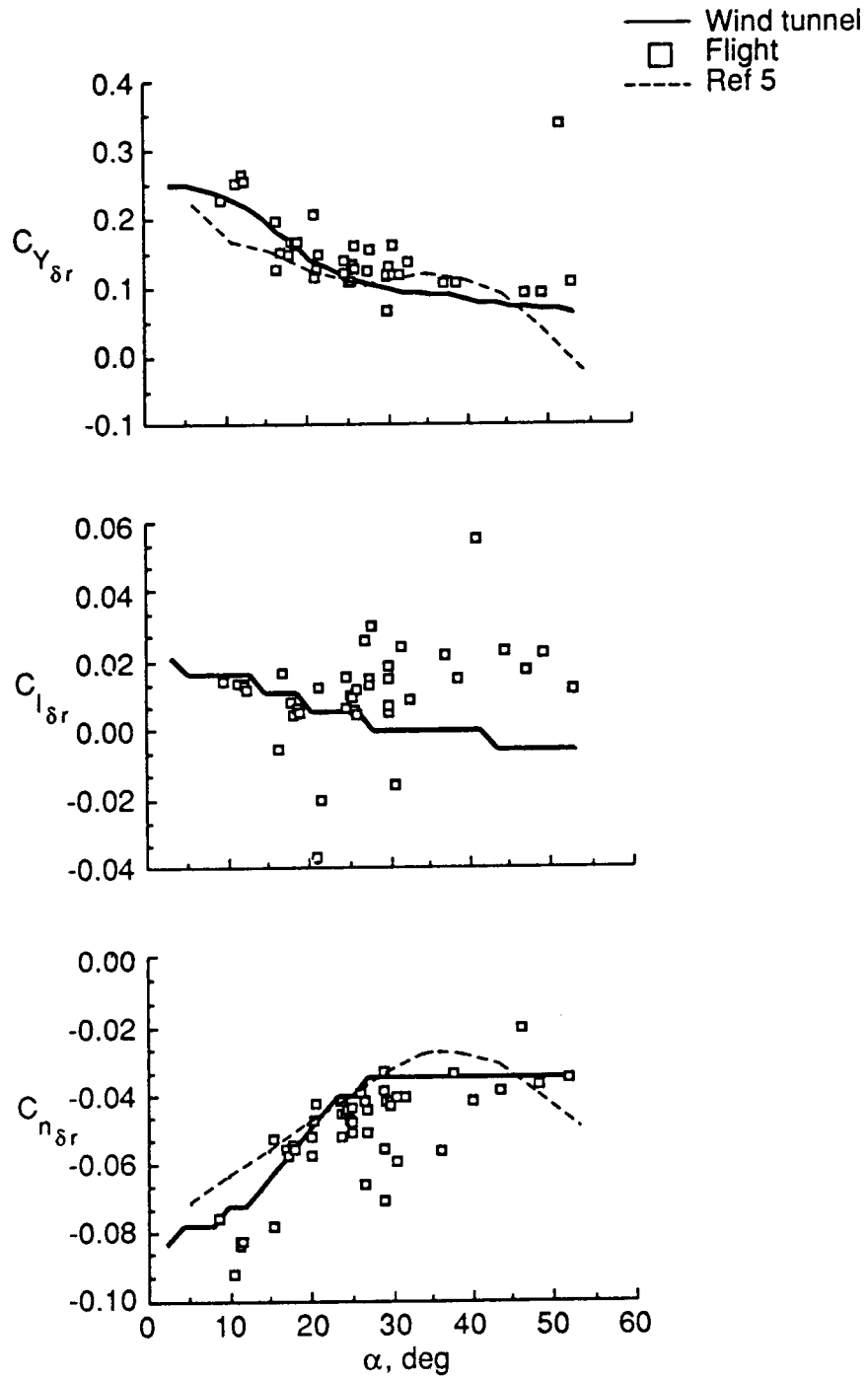   obtained from flight and wind tunnel
            measurement.

40
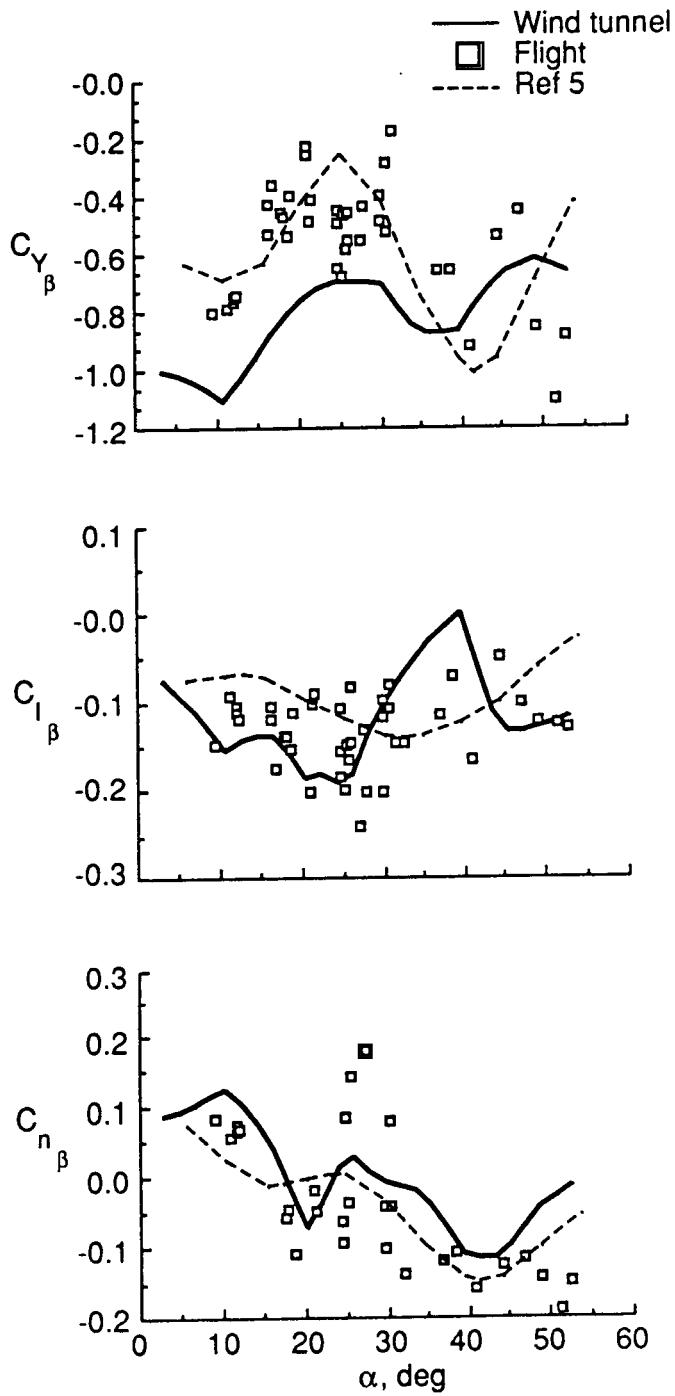
Figure 12. Comparison of parameters expressing sideslip effect estimated from flight and wind tunnel measurement.

41
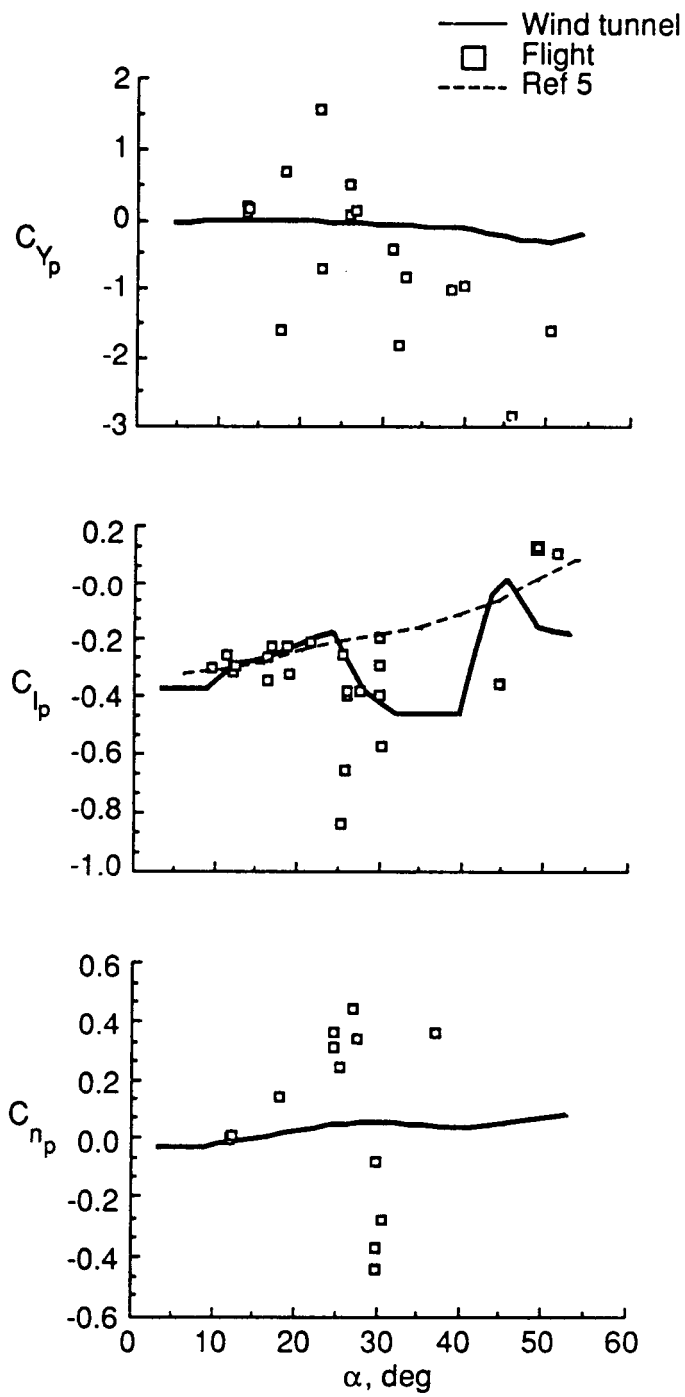
Figure 13. Comparison of oscillatory roll-rate para-
meters estimated from flight and wind tunnel
measurement.
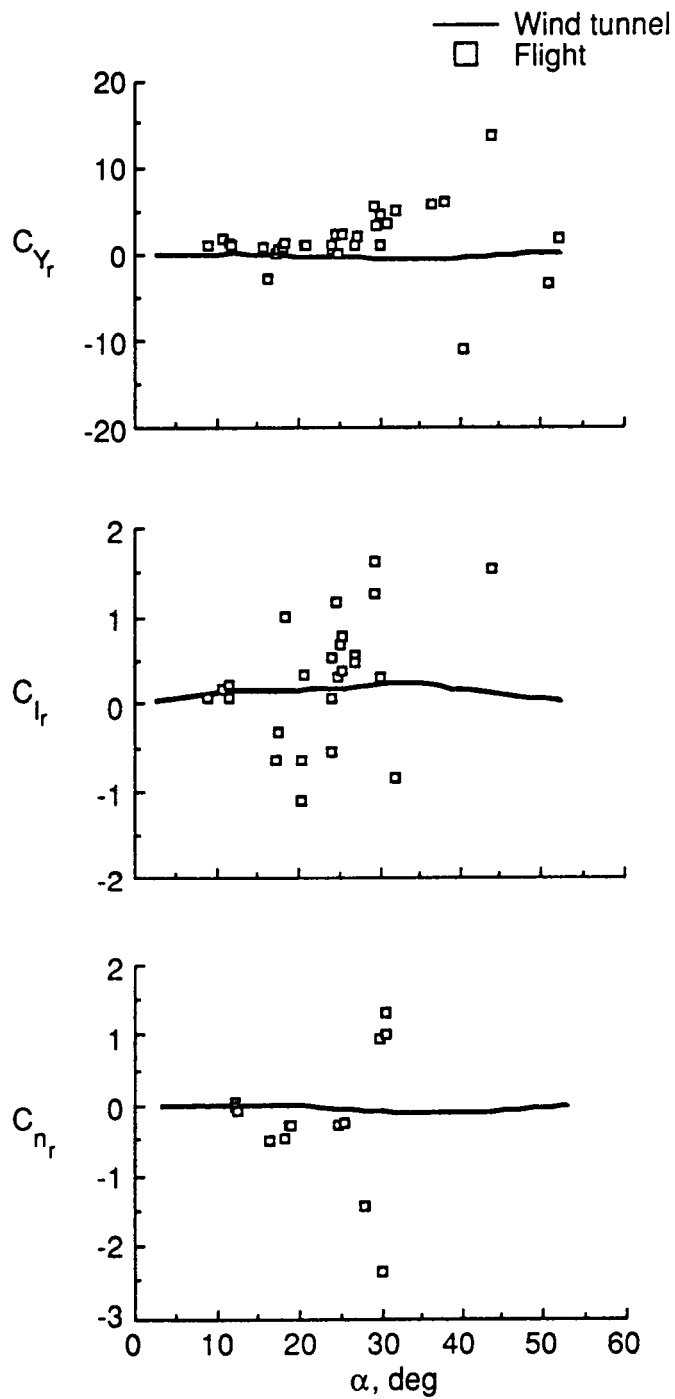
Figure 14. Comparison of oscillatory yaw-rate parameters
from flight and wind tunnel measurement.
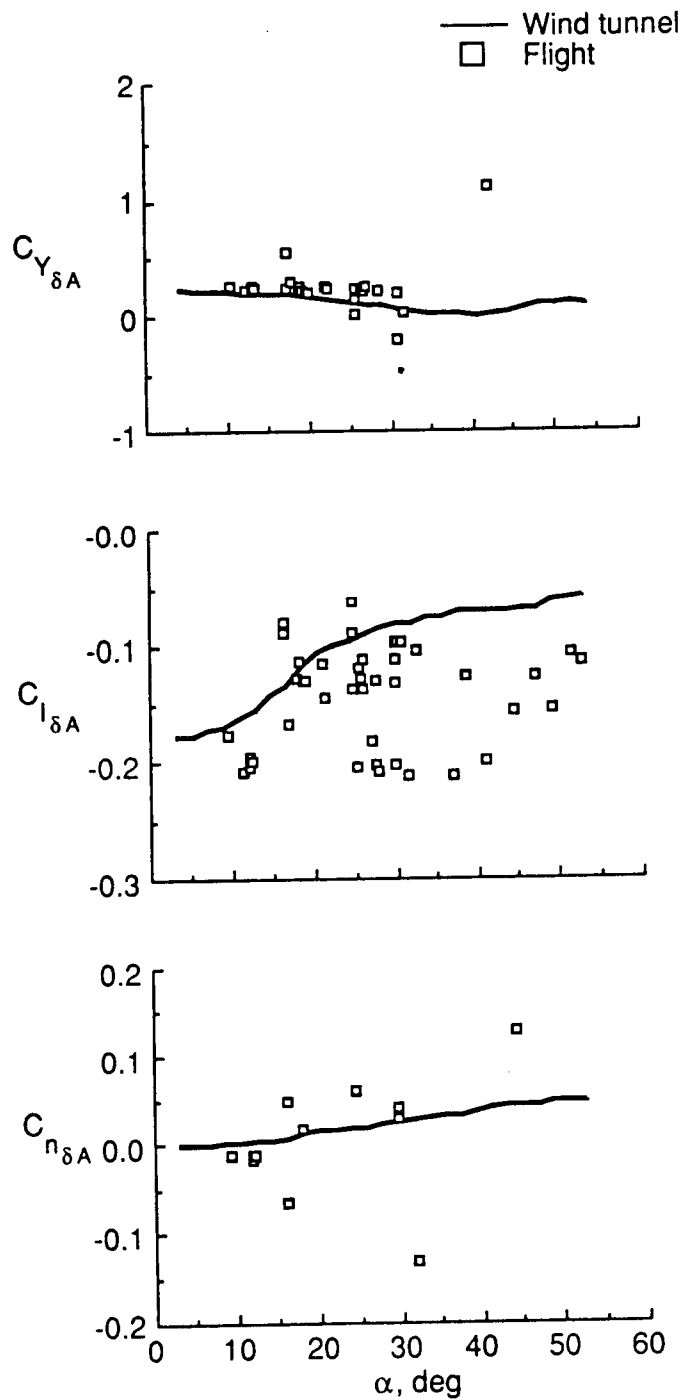
Figure 15. Comparison of aileron-effectiveness parameters estimated from flight and wind tunnel measurement.

44

Figure 16. Comparison of rudder-effectiveness parameters estimated from flight and wind tunnel measurement.

45
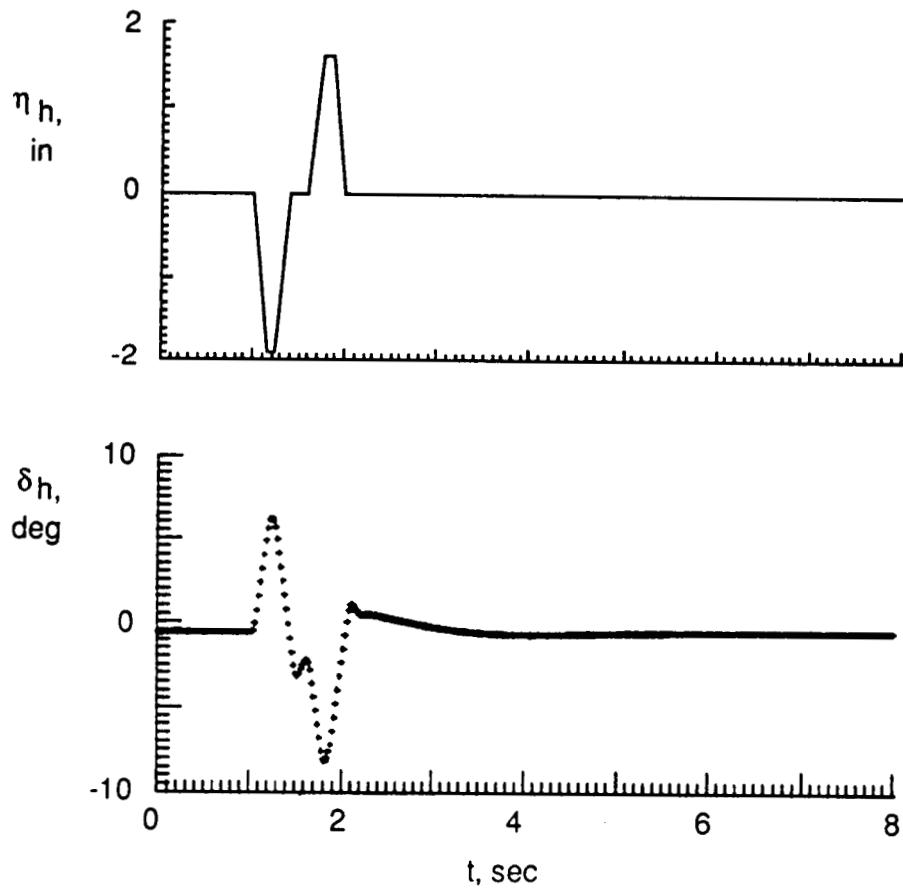
Figure 17.   Time histories of flight inputs and simulated
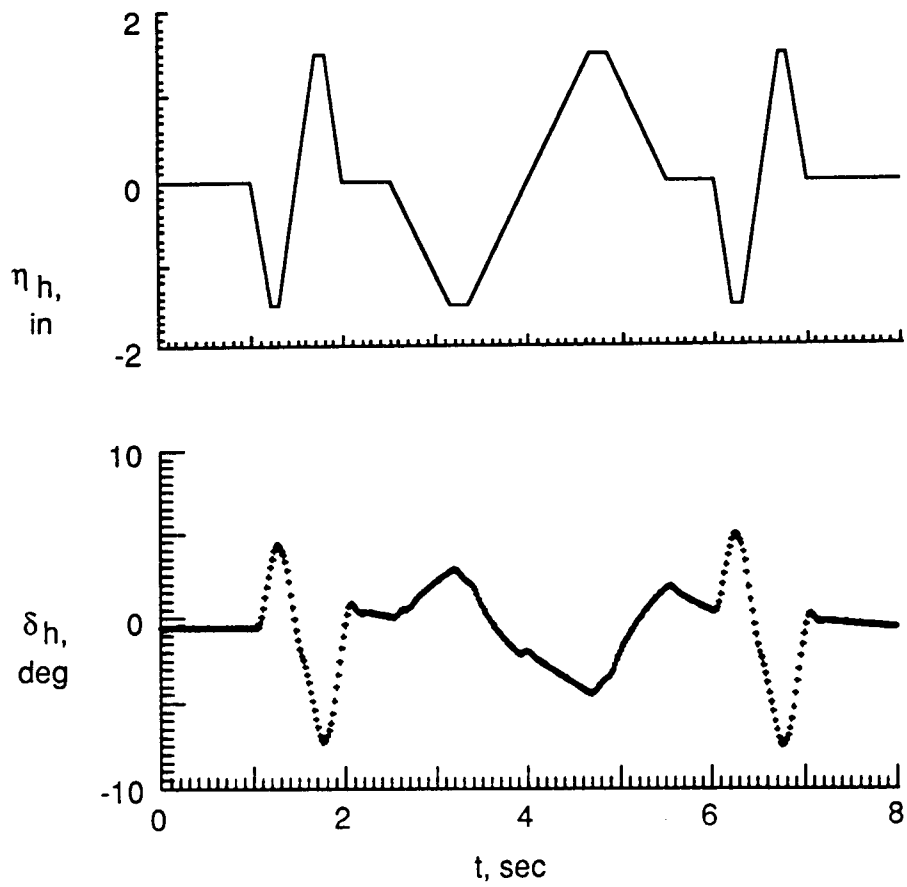longitudinal response variables.
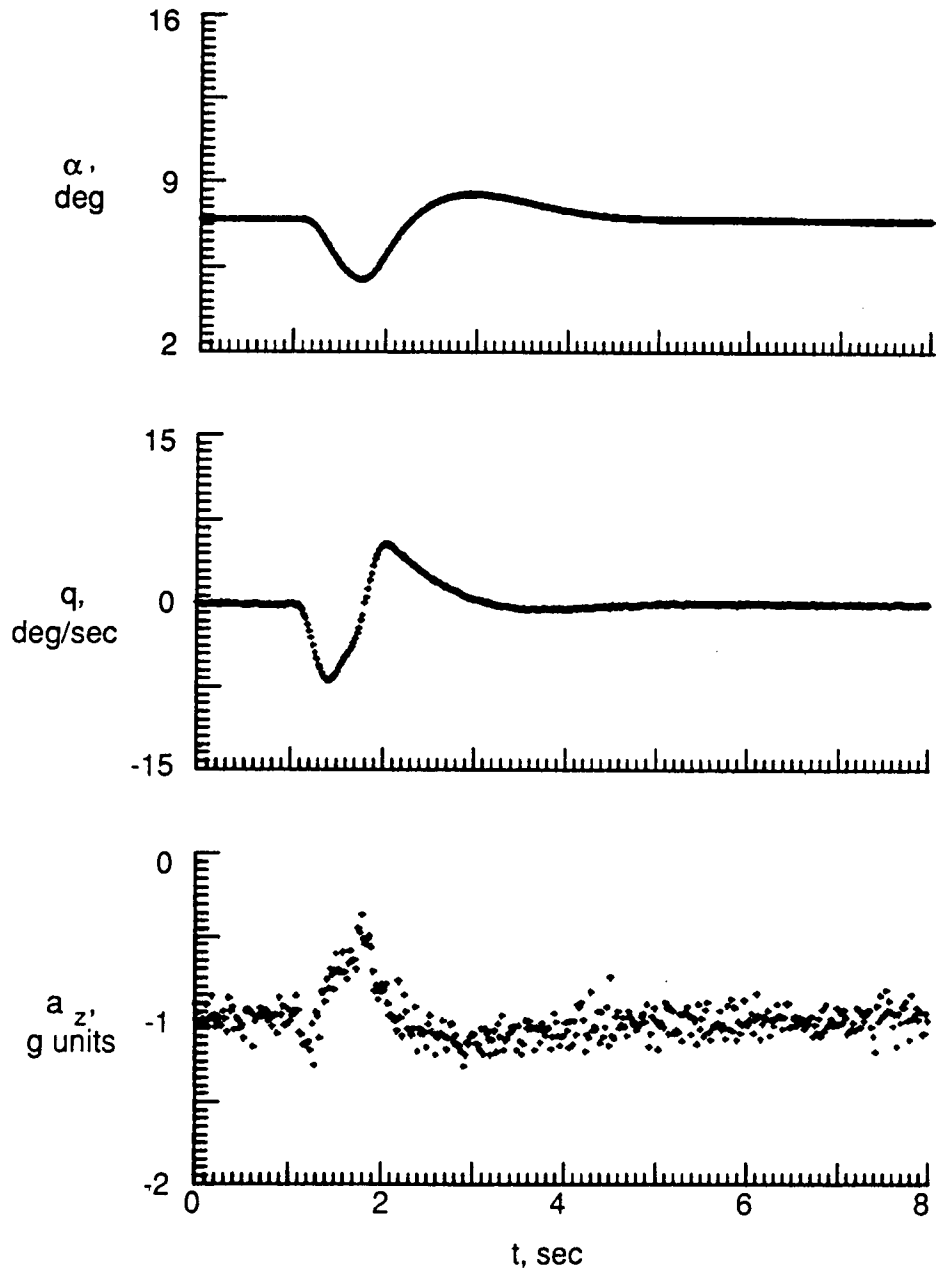
Figure 17. Concluded

47

Figure 18. Time histories of selected inputs and simulated longitudinal response variables.
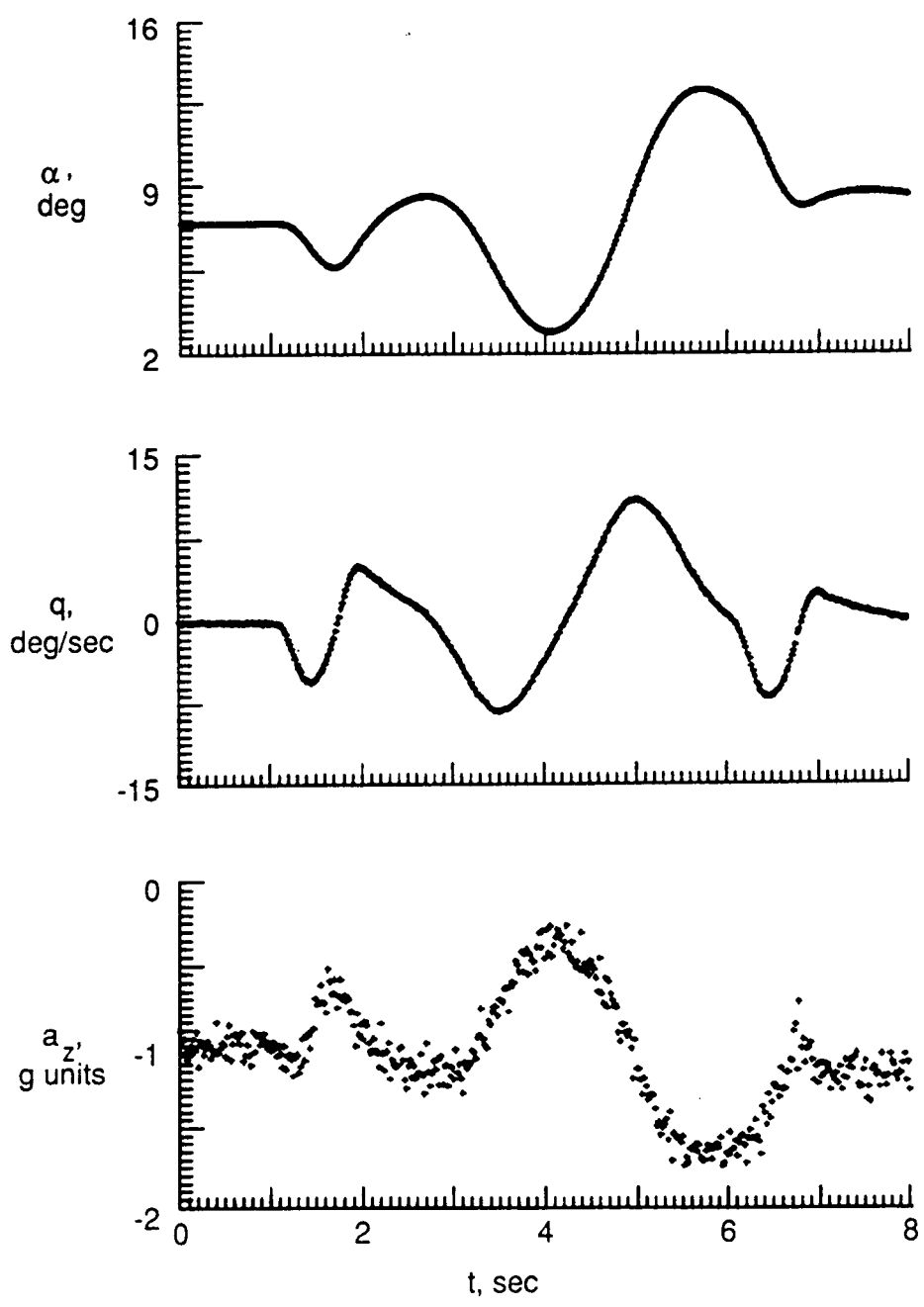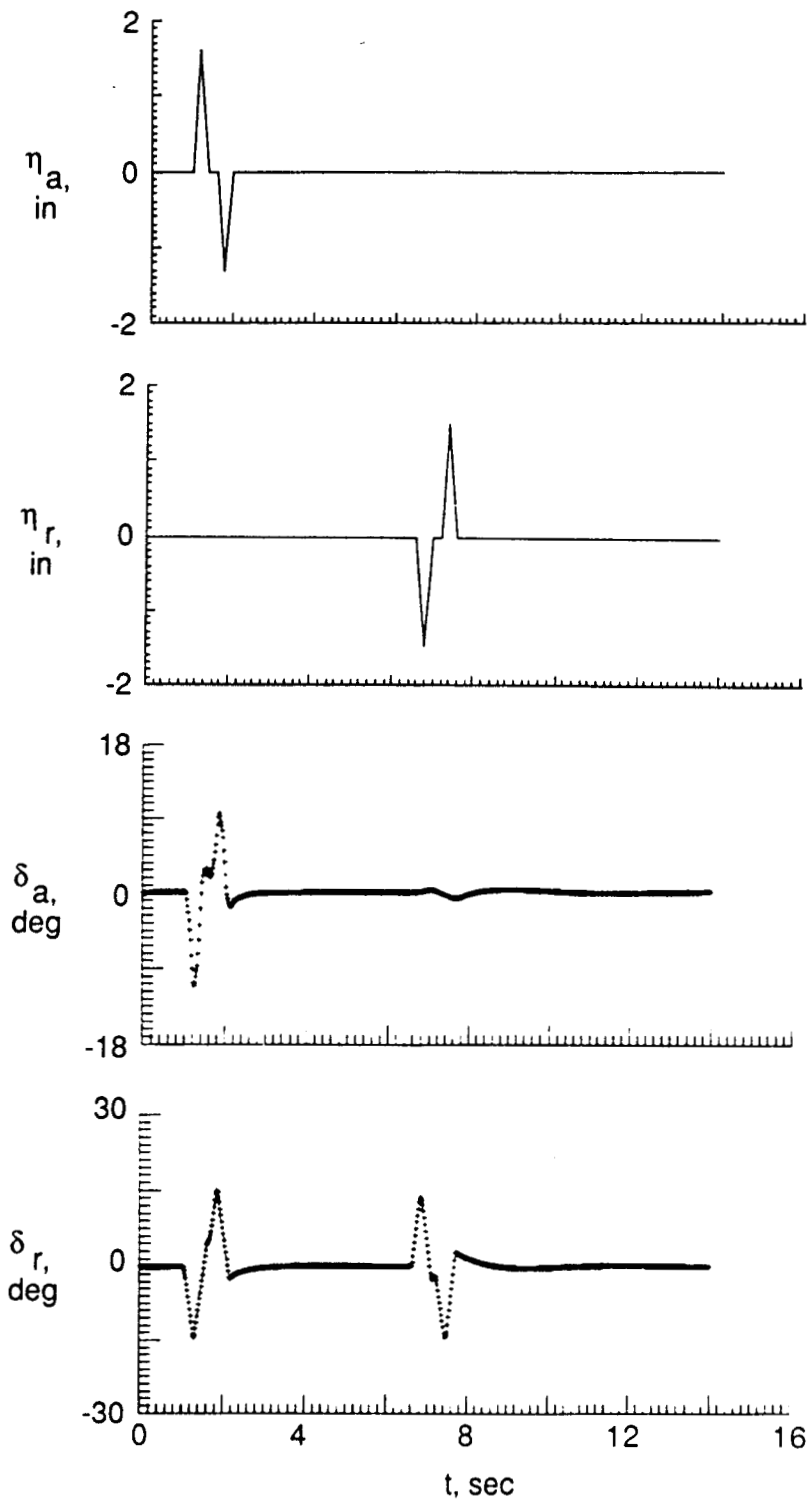
48

Figure 18. Concluded

Figure 19.   Time histories of flight inputs and simulated
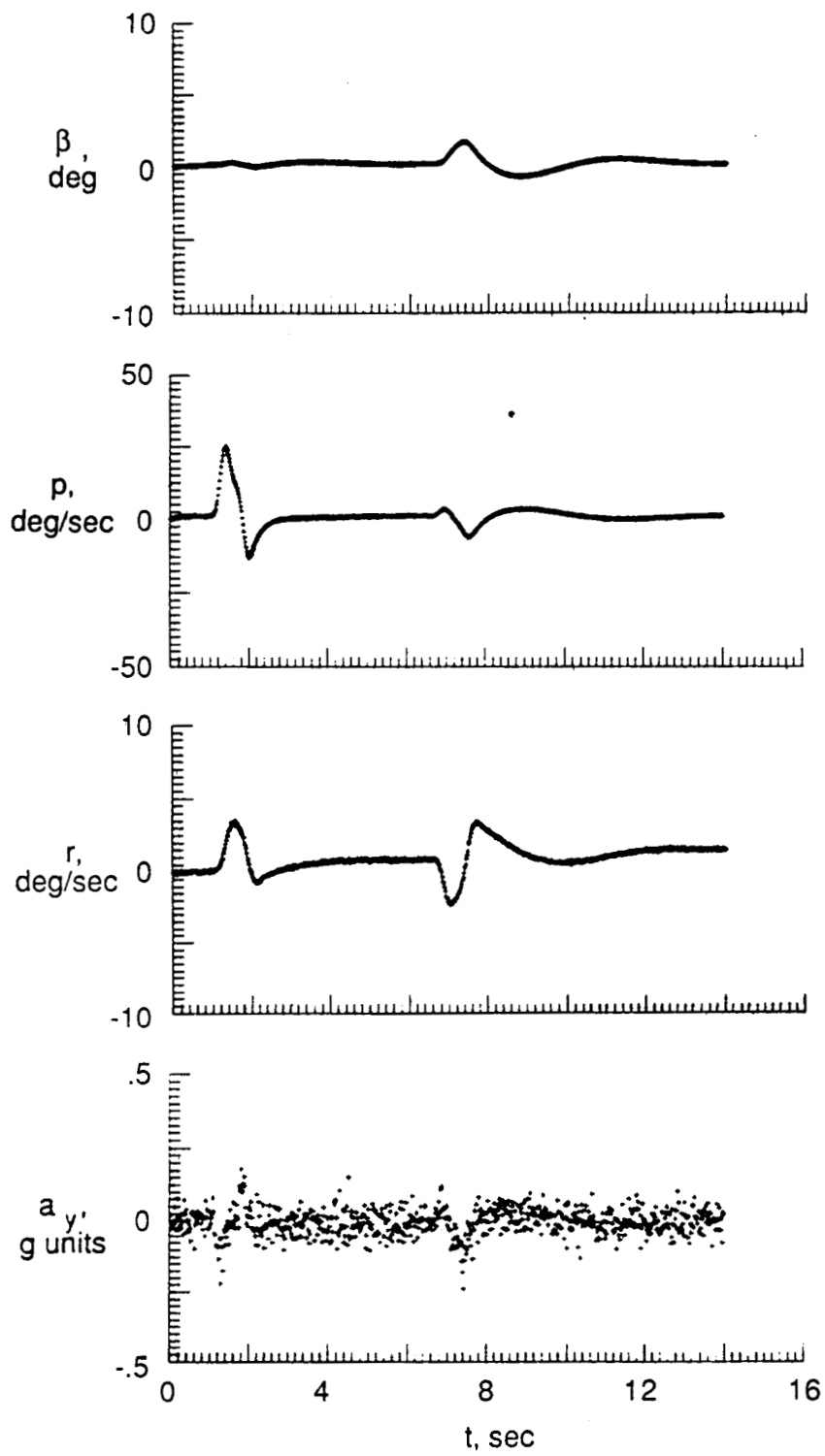lateral response variables.

Figure 19. Concluded

51

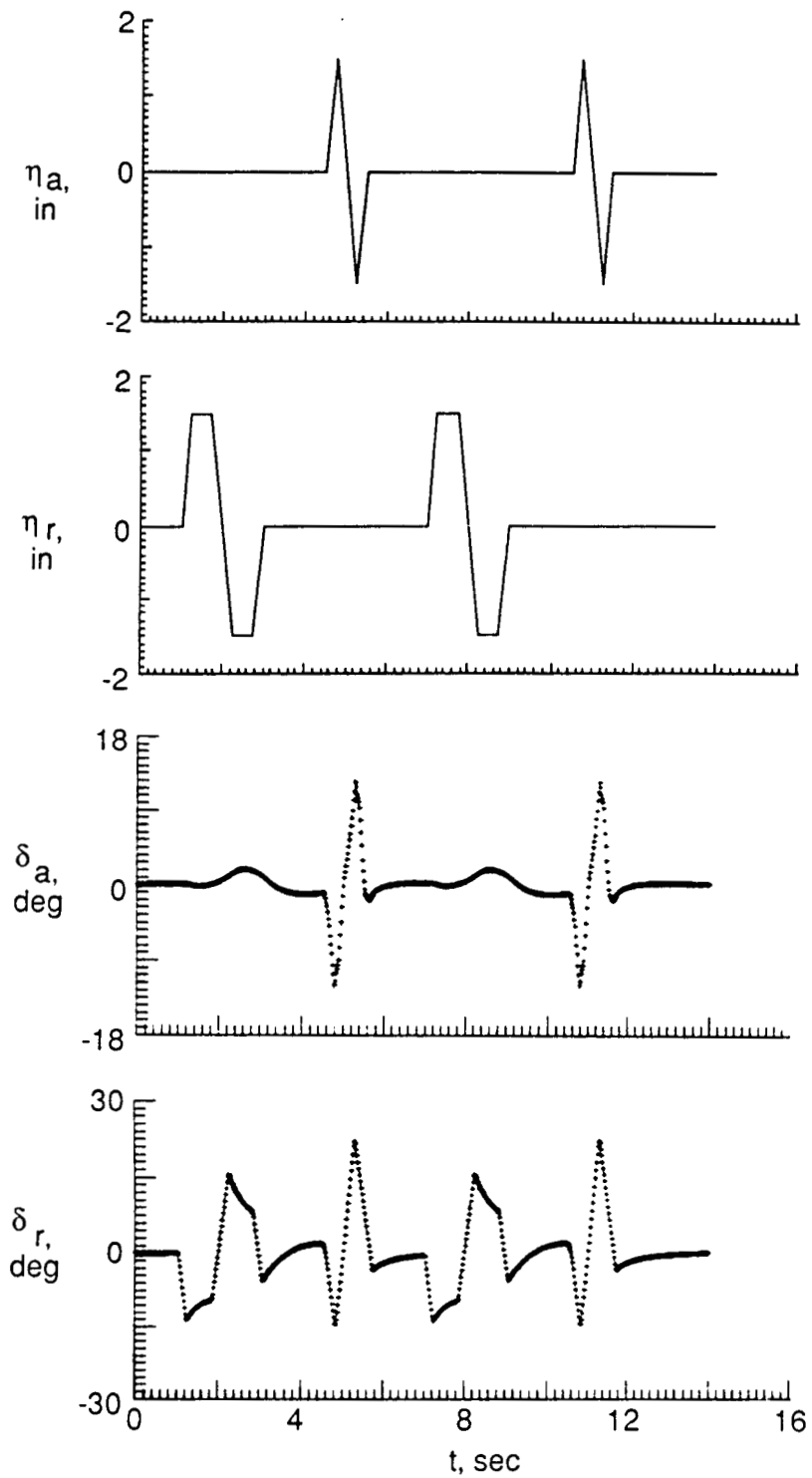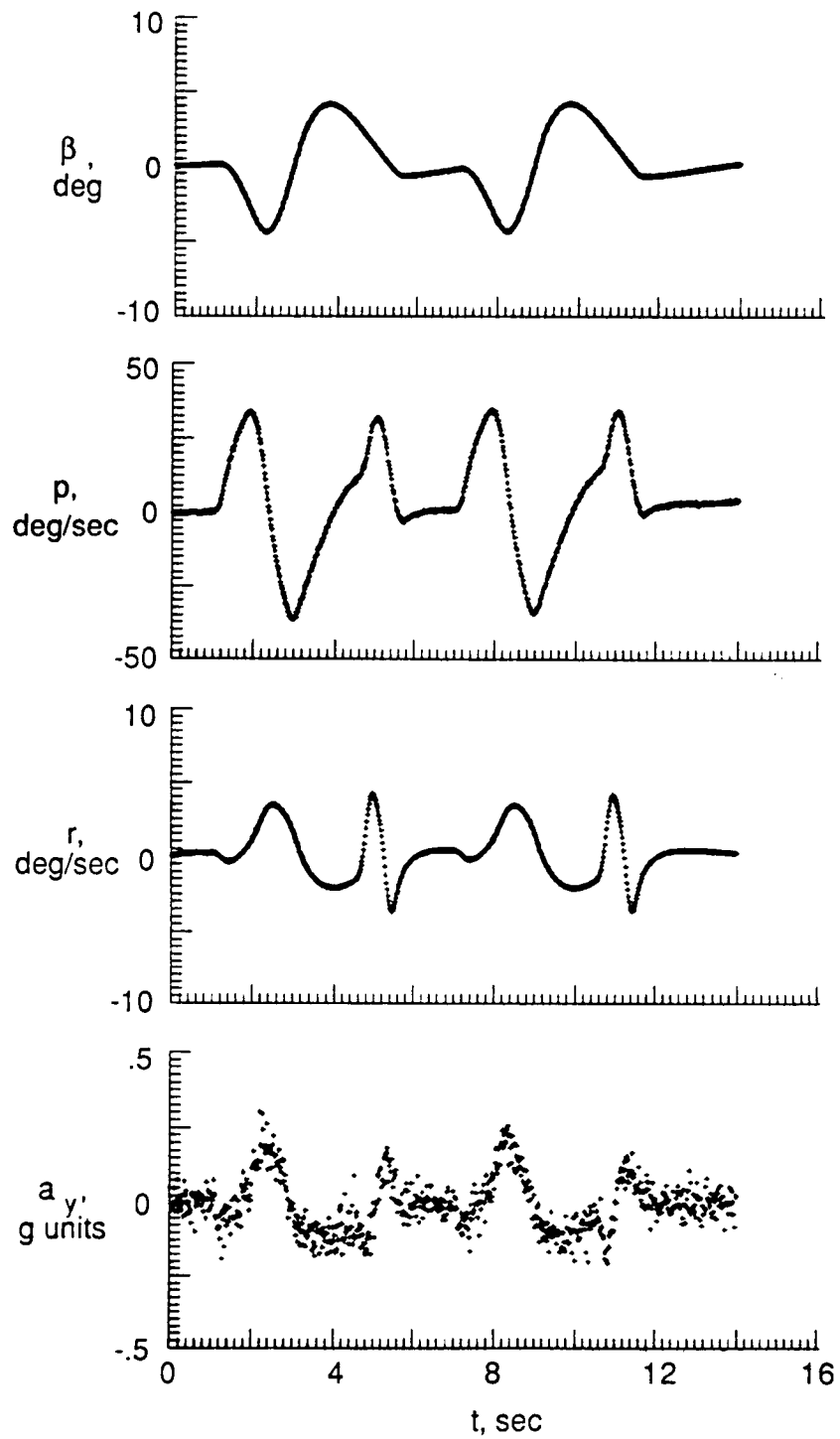Figure 20. Time histories of selected inputs and simulated lateral response variables.

Figure 20. Concluded

NASA
National Aeronautics and Space Administration

Report Documentation Page

1. Report No. NASA TM-101631	2. Government Accession No.	3. Recipient's Catalog No.

4. Title and Subtitle	5. Report Date
Aerodynamic Parameters of an Advanced Fighter Aircraft Estimated from Flight Data. Preliminary Results	July 1989
	6. Performing Organization Code

7. Author(s) Vladislav Klein, Keven P. Breneman, and Thomas P. Ratvasky	8. Performing Organization Report No.
	10. Work Unit No. 505-66-01-02

9. Performing Organization Name and Address NASA Langley Research Center Hampton, VA 23665-5225	11. Contract or Grant No.
	13. Type of Report and Period Covered TECHNICAL MEMORANDUM
12. Sponsoring Agency Name and Address National Aeronautics and Space Administration Washington, DC 20546-0001	14. Sponsoring Agency Code

15. Supplementary Notes

Vladislav Klein, Keven P. Breneman, and Thomas P. Ratvasky: The George Washington University, Joint Institute for Advancement of Flight Sciences, Langley Research Center, Hampton, Virginia.

16. Abstract

Preliminary estimates of aerodynamic parameters of an advanced fighter aircraft were obtained from flight data of different values of the angle of attack from 8° to 54°. The data were analyzed by a stepwise regression with the ordinary least squares technique. The estimated stability and control derivatives are plotted against the angle of attack and compared with wind tunnel measurement and previous flight results. The report also includes the data compatibility check of measured data. The effect of various input forms on the estimates is demonstrated in two examples using simulated data.

17. Key Words (Suggested by Author(s)) parameter estimation linear regression data compability input forms	18. Distribution Statement UNCLASSIFIED - UNLIMITED Subject Category 08

19. Security Classif. (of this report) UNCLASSIFIED	20. Security Classif. (of this page) UNCLASSIFIED	21. No. of pages 58	22. Price A04

NASA FORM 1626 OCT 86